Use of electrophoretic impregnation and vacuum bagging to impregnate SiC powder into SiC fiber preforms

Binner, Jonathan; Vaidhyanathan, Bala; Jaglin, David; Needham, Sarah

DOI:
10.1111/ijac.12143

International Journal of Applied Ceramic Technology
Ceramic Product Development and Commercialization

Use of Electrophoretic Impregnation and Vacuum Bagging to Impregnate SiC powder into SiC Fiber Preforms

Journal:	*International Journal of Applied Ceramic Technology*
Manuscript ID:	ACT-2148.R1
Manuscript Type:	Article
Date Submitted by the Author:	n/a
Complete List of Authors:	Binner, Jon; Loughborough University, Materials; Vaidhyanathan, Bala; Loughborough University, Materials Jaglin, David; Loughborough University, Materials Needham, Sarah; Rolls Royce plc, Civil Small & Medium Engines
Keywords:	infiltration, silicon carbide, composites, fibers

Use of Electrophoretic Impregnation and Vacuum Bagging to Impregnate SiC powder into SiC Fiber Preforms

Jon Binner*, Bala Vaidhyanathan, David Jaglin and Sarah Needham†

Department of Materials, Loughborough University, Loughborough, Leicestershire LE11 3TU, United Kingdom

Abstract

Techniques based on vacuum bagging (VB) and electrophoretic impregnation (EPI) have been investigated for the impregnation of SiC powder into layered Nicalon SiC fabric preforms. The aim was to produce pre-impregnated samples for subsequent chemical vapour infiltration (CVI) with reduced intertow porosity that arises from the construction of the fabric layers whilst leaving unblocked the intratow porosity that is so indispensable for a successful infiltration. Since the goal was simply to learn about the ability to impregnate the samples, no interphase coating was applied to the fibers as would normally be used when producing SiC_f-SiC composites. Whilst the VB process generally yielded much stronger preforms, depending on the pressure used and the powder particle size, it resulted in powder becoming located in the intratow rather than the intertow porosity. In contrast, provided an appropriate electrode arrangement was used, EPI offered the potential for a more controlled impregnation process with the powder primarily found in the intertow porosity; however, the preforms were very weak and delaminated easily. The combination of the two processes resulted in a very successful approach, with greater uniformity of particle infiltration and higher green strengths, whilst largely avoiding impregnating the intratow porosity.

* J.binner@Lboro.ac.uk
† Now with Rolls Royce plc., UK

I Introduction

SiC_f/SiC composites are very promising materials for high temperature structural applications because of their good thermal stability and excellent mechanical properties. Of the various techniques used to produce fiber reinforced ceramic matrix composites, chemical vapour infiltration (CVI) has received considerable attention[1-2]. Combining isothermal or temperature gradient, isobaric or pressure gradient features, as well as the use of pulsing, CVI results in composites still containing 10 - 20% residual porosity[3-6] however. This is mainly due to two reasons: (i) when the minimum percolation threshold for transport through the pore structure is reached, infiltration becomes more and more difficult as the pore size decreases resulting in deposition occurring on the outside of the fiber network, and (ii) when the composite reaches a fractional density of ~70% the surface area becomes dominated by the macropores; these can take too long to infiltrate from a commercial viewpoint. It is the last 30% of densification that is financially costly because the infiltration time becomes extended (to days and even weeks in some cases) during this phase[7] and to produce fiber-reinforced ceramic matrix composites (FRCMCs) by any form of CVI at a commercially acceptable cost, the processing time must be kept short[8].

As implied above, the porosity itself can be divided into two main types; fine intratow and much larger intertow porosity. In fibrous preforms densified up to 82% of theoretical[9], the lamination of the plies combined with the weave design can result in intertow pores being as large as 0.3 to 0.6 mm in width and tens of millimetres long. There is also the problem of the packing of the fabric layer in the Z-direction[10]. Fig. 1a[11] provides an illustration of this type of porosity, which is the most harmful type of defect for mechanical properties as well as providing a path for corrosive agents. When present, these pores are very difficult to eliminate in fiber preforms produced from the lay-up of fiber sheets. In contrast, intratow pores are typically <15 μm in diameter and are formed when the matrix deposition on the individual fibers traps small pores,

Fig. 1b. Whilst some will probably always be residual after CVI-based processes, they are not considered to be particularly detrimental to the overall strength of the composite due to their small size[9]. Nevertheless, the elimination of this porosity by the use of the right infiltration conditions would also undoubtedly be desirable – provided it can be achieved without a significant increase in processing time and hence costs.

Two-stage CVI processes have therefore been investigated where, under the right conditions, the initial stage sees the efficient filling of the finer, intratow porosity and the second stage seeks to fill as much of the coarser, intertow pores as possible within the economic limitations of the process[12-13]. For example, using marker layers, Lackey *et al.*[14] found that when using forced-flow CVI, intratow infiltration could be virtually complete within the first 2 h, although filling the intertow porosity took considerably longer. One potential problem with this approach is that some intertow porosity can become trapped in the structure when the intratow porosity becomes filled.

Although not the focus of this paper, many other techniques are available for the fabrication of FRCMCs as well as CVI. For example, hot-pressing techniques have been used[15] in which the stacked green body was hot-pressed at up to 2023 K with a matrix consisting of β-SiC powder and sintering aids. Unfortunately, the composite displayed brittle behaviour even though Hi-Nicalon fibers were used. An approach based on slurry-cast melt infiltration with reaction-sintering[16-18] used a slurry consisting of SiC powder or a mixture of SiC powder and carbon powder in water that was impregnated into the SiC fiber preform. The green composite was then reaction sintered at 1720 K with melted silicon to obtain a rich SiC matrix. Disadvantages lay in the need for a designed mould and residual silicon metal as high as 15-20 vol.%, despite the low porosity achieved.

An alternative approach can be based on the pre-impregnation of the macropores by a process

other than CVI and polymer impregnation and pyrolysis (PIP) processes are very common and effective manufacturing techniques for high performance SiC_f/SiC composites[19-24]. Six or more cycles of impregnations, followed by the pyrolysis, are typically required to achieve densities of 80-85%. An important aspect of the process is that the matrix development affects the mechanical properties by inducing residual stresses due to shrinkage of the matrix during pyrolysis and also the anisotropy of the thermal expansion coefficient between the fibers and matrix[25].

The introduction of powder into the PIP was investigated by Gonon and Hampshire[21] who used polysilazane as precursor with the addition of Si_3N_4 powder into SiC fiber preforms; 7 to 8 cycles of precursor impregnation and pyrolysis were required to reduce the porosity to approximately 15%, but the presence of powder did not allow good cross-linking of the precursor and resulted in lower mechanical properties than the composite with the polymer alone, a result confirmed by Casadio[23]. Gotoh *et al.*[20] also pointed out that optimisation of the mechanical properties relies on the right volume of fiber and sintering aids. Fast heating techniques such as microwaves can be applied during the pyrolysis stage, providing time and energy savings since suitably high temperatures can be induced in a matter of minutes. Dong and co-authors[24] used this particular technique but required 8 cycles of impregnation to achieve a final density of 78%.

Combining PIP with CVI allowed Kim *et al.*[22] to achieve an initial preform density of up to 70% after PIP, the subsequent isobaric, isothermal CVI step yielding a composite density of 82%. Ortona *et al.*[10] found that an initial CVI stage can prevent the swelling of the preform during the PIP stages.

Two simple and rapid processes that have been shown to lead to a successful pre-impregnation in other, non-SiC fiber-based systems are vacuum bagging (VB) and electrophoretic

impregnation (EPI). VB is a relatively simple process that was developed by Rolls Royce in the 1980s for the preparation and/or repair of polymer matrix carbon fiber composites in the aerospace industry[26-28]. This technique has subsequently been modified for the impregnation of ceramic powders between tows and layers of fiber-based fabrics in order to reduce the porosity and improve the green strength[29]. The fabric layers are individually coated with ceramic slurry and stacked, prior to being dried and consolidated under vacuum. Process parameters are mainly associated with the preparation of the slurry, which controls the particle size being used and the amount of powder to be impregnated, and the pressure involved during vacuum bagging.

EPI is directly related the electrophoretic deposition process (EPD) wherein charged particles are deposited on an electrode surface via their migration under the action of an electrical field[30]. In the EPI process, a fiber preform is impregnated via the deposition of particles from a slurry onto individual cloth layers prior to assembly into the preform. The movement of ceramic particles in a suspension within an electric field is governed mainly by factors such as the field strength[31], the pH of the suspension and its ionic strength[32]. The amount of polyelectrolyte addition also influences the rate of deposition and the homogeneity of the deposited material[33]. Green composite microstructures with good infiltration uniformity and few macro defects have been obtained by this technique[34-35] and previous work with a SiC_f/SiC system resulted an increase in density from 20 vol.% (the initial fiber preform density) to over 40 vol.% in only 20 minutes[36].

In the present work, a methodical examination of the use of stand-alone VB and EPI techniques as well as their combination with a number of geometrical modifications has been undertaken with a view to producing SiC powder-loaded SiC fiber preforms that are suitable for subsequent infiltration with a SiC matrix using CVI. The goal was to fill the larger intertow pores, so reducing

the time that would be needed during a subsequent CVI stage, whilst avoiding the introduction of powder particles within the tows themselves. The particles can cause abrasion during use and damage the tows. In addition, it was desired to produce impregnated fiber preforms that were mechanically robust and capable of being handled prior to and during the CVI stage.

II Experimental procedure

(1) Materials

The preforms were made from NL-202 SiC fibers (Nippon Carbon, Tokyo, Japan) woven (by Sigmatex Ltd., UK) into a 2D plain weave NP1616 pattern. Forty eight mm circular discs were cut from the cloth using a metal template and ceramic scissors. The sizing agent was removed by heating the fiber discs in a furnace at 600°C for 2 h. Note, no attempt was made in this work to apply an interphase coating to the fibers prior to undertaking the impregnation with powder particles. This was because it was not believed that such a coating would materially affect the identification of the best choice of impregnation process, which was the goal of this work. For the impregnation experiments themselves, five SiC powders with mean particle sizes of approximately 0.6, 2.5, 6.7, 10.0 and 12.8 μm were used; their details are provided in table 1.

(2) SiC powder slurry preparation

Three types of slurries were prepared. Slurry A was used during the impregnation of preforms by vacuum bagging (VB), whilst slurries B and C were used for electrophoretic impregnation (EPI) and gravitational settling (GS).

Slurry A: Aqueous slurries containing solids loadings between 20 and 40 vol.% were prepared for all five of the SiC powders. The powders were dispersed using 1 to 1.5 wt.% of Glascol K11 (Ciba Speciality Chemicals, Bradford, UK) and the pH was fixed at 9.0 ± 0.2 via the addition of ammonia solution. To eliminate powder agglomerates, the slurries were ball-milled in airtight

polyethylene bottles using zirconia media for 24 h, the viscosity being regularly monitored. Note that, although slurries with a solid loading higher than 45 vol.%, were prepared, problems were experienced with subsequent wetting of the fiber fabric and hence these slurries were discarded.

Slurry B: Ethanol-based slurries containing solids loadings of 5 and 10 vol.% were prepared for four of the SiC powders, the powders being dispersed using 0.5 vol.% of triethylamine (Ciba Speciality Chemicals, Bradford, UK); the pH was 9.0 ± 0.2. The 12.8 μm SiC powder was not used as it was found that particle migration was difficult to achieve at the voltages used. To remove powder agglomerates, during preparation the slurries were exposed to ultrasonic energy at 23 kHz (Soniprep 150 Ultrasonicator, MSE Scientific Instruments, Manchester, UK) for a minimum of 60 s together with mechanical agitation using a magnetic stirrer.

Slurry C: An identical preparation route as for slurry B was used to prepare aqueous suspensions containing 5 vol.% of SiC powders for all five of the SiC powders, again with the addition of ~0.5 vol.% of triethylamine. The pH was again 9.0 ± 0.2. Ultrasonic energy and mechanical agitation was again used, as described for slurry B.

(3) Vacuum bagging

A small amount of slurry A was applied to the discs of SiC fabric using a nylon brush. Since the impregnation of the powder was performed manually, the VB technique potentially lacked repeatability with respect to the amount of powder deposited on each fabric layer. To minimise this problem each layer was weighed after brushing to ensure that a consistent amount had been deposited. Ten discs were then stacked and the layers compressed using a roller. Each preform was placed in the vacuum bagging equipment (Townsend & Mercer Ltd., Croydon, UK), Fig. 2a, and dried overnight at temperatures ranging from 20 to 60°C, a rotary pump being used to apply a vacuum of ~0.5×10^5 Pa. The combination of the pressure used and drying process meant that the stack of disks held together sufficiently for subsequent handling.

(4) Electrophoretic impregnation and gravitational settling

Fig. 2b is a schematic diagram of the experimental arrangement used for the electrophoretic impregnation process. Initially, flat stainless steel plates were used as electrodes, Fig. 3a, placed vertically in the suspension 15 mm apart. The fiber preforms were attached to the anode since gas formed at the cathode that could have become trapped in the green compact. Two further electrode systems were devised following the initial results with the vertical electrodes, these being (i) vertical electrodes accommodating a rotating device for the anode, Fig. 3b, with speeds from 0 to 6 rpm and (ii) horizontal electrodes, Fig. 3c. The latter were also used without an electric field for comparative work involving the gravitational settling (GS) of particles. The authors are not aware of any previous work in terms of impregnating fiber preforms using simple gravitational settling; it was used simply to get a feel for how important the electrical field was.

For each impregnation a fabric disc measuring 48 mm diameter was laid on top of the appropriate anode and a polypropylene (PP) mask the same size as the electrode clamped over it using plastic grips. The PP cover had a 40 mm internal diameter opening cut in it to allow impregnation to occur into the preform; it should be noted that this design prevented any deposition of SiC powder in the outer 4 mm of the preform. Electrophoretic impregnations were carried out by applying a potential difference ranging from 50 to 100 V in constant voltage mode using slurries B and C. Each fabric disc was processed and the anode wiped clean of slurry before the next disc was attached on top of the previous, wet disc. The whole process was performed as fast as possible and the stack of ten powder impregnated discs was then allowed to dry overnight at room temperature. For all of the EPI-based processes, the final drying stage provided some strength to the stack of disks but they needed very careful handling.

For the gravitational settling (GS) process, the horizontal anode was used with no applied field. Each fabric disc was mounted on the anode as for the EPI process and held in place by the PP

cover. The slurry was stirred and, the moment the stirring stopped, the anode was plunged to the bottom of the beaker containing the suspension for a set period of time. The anode was then removed from the beaker and a fresh fabric disc placed in position on top of the wet one and the process repeated until a preform consisting of ten discs had been produced. Once again, the stack of discs produced needed very careful handling to prevent them delaminating.

(5) Combined process

Fabric discs were initially infiltrated with slurries B and C using the EPI and GS processes and then subsequently consolidated using the VB process as described previously. The use of the latter provided adequate strength to the stack for subsequent handling.

(6) Characterisation

Specimen diameters and thicknesses were measured using a vernier calliper gauge. The relative fiber volume, V_f, and relative powder volume, V_p, of the preforms (as a percentage of the total preform volume) were determined from the mass of the preform prior to powder impregnation, m_f, and its mass after powder impregnation, m_s, (from which the mass of powder impregnated, m_p, could be calculated) and the actual volume of the preforms, V_s, the latter being calculated from its geometry:

$$V_f = \frac{m_f}{V_s \rho_f} \times 100 \text{ (\%)} \quad \textbf{(1)}$$

$$V_p = \frac{(m_s - m_f)}{V_s \ \rho_{\text{SiC}}} = \frac{m_p}{V_s \ \rho_{\text{SiC}}} \times 100 \text{ (\%)} \quad \textbf{(2)}$$

where ρ_f is the density of NL-202 Nicalon fiber (2.55 g cm^{-3}) and ρ_{SiC} is the density of stoichiometric SiC (3.21 g cm^{-3}).

Assessment of the efficiency of the different processes was achieved by calculating the void reduction:

$$V.R. = (1 - \frac{100 - (V_f + V_p)}{100 - V_f}) \times 100 \text{ (\%)} \quad \textbf{(3)}$$

Comment [JB1]: Equation corrected (extra pair of brackets inserted).

Scanning electron microscopy was used to study both the powder distribution across the sample and the level of impregnation into the intratow and intertow porosity. The use of secondary and backscattered electron imaging allowed the powder additions to be differentiated with clarity from the fibers.

Dual energy X-ray absorptiometry (DEXA) also provided information on the powder distribution after impregnation. A Lunar DPX-L DEXA was calibrated for SiC materials[11] and photon attenuation maps acquired which, particularly when artificially coloured, provided a clear, qualitative representation of density variations across the diameter of the specimens.

Using Darcy's law for laminar viscous flow in porous materials[37], the gas permeability of the samples, *K,* was calculated by plotting the ratio of the pressure difference across the sample thickness against the airflow. This provided a rough measure of the permeability of the preforms, with a view to ensuring that a subsequent CVI process would be capable of occurring. The pressure drop, ΔP, across the preforms (thickness L) was measured from the difference between the inlet and outlet pressure in a permeability rig similar to that described elsewhere[38]. The viscosity of the air was taken as $\mu_{air} = 1.827 \times 10^{-5}$ Pa s.

III Results & Discussion

As indicated above, the primary aim of the impregnation experiments was to reduce the intertow ~~porosity~~ pore sizes of the preform, in order to shorten a subsequent chemical vapour infiltration process (not reported in this work), whilst ensuring that the preform has enough green strength

to allow handling and that the intratow porosity was accessible for infiltration. The distribution of the powder in the intertow and intratow porosity, as well as the uniformity of its distribution across the fiber preform, were therefore of key importance.

Throughout the results, including Tables II – IV, the samples are identified by a code in which the first letter(s) is indicative of the impregnation system used; V for vacuum bagging, E for electrophoretic impregnation, G for gravitational settling, EV for combined electrophoretic impregnation and vacuum bagging and GV for combined gravitational settling and vacuum bagging.

(1) Vacuum bagging

The vacuum bagging results are shown in Table II and Fig. 4. As expected, it can be seen that the amount of powder impregnated into the preforms (indicated by the values of V_p) was mainly influenced by the solids loading of the slurry, rather than the particle size. Repeatability of the results were confirmed with similar samples displaying V_p values (and hence V.R. and relative density values) ~~of ±1%~~within ±1% variation. SEM analysis revealed that compaction of the layers occurred with the intertow ~~porosity~~ pores being reduced to typically 50-100 μm wide (the uncompacted intertow pores were up to ~500 μm wide). When the solids loading was ≥30 vol.% the particles systematically infiltrated these intertow voids leaving only a few, small regions unfilled, Fig. 5a. In contrast, when a 20% slurry was used very little intertow powder impregnation occurred, Fig. 5b, with just a little localised impregnation. For all solids contents, impregnation of the tows occurred for the 0.6 and 2.5 μm particle sizes as the pressure and vacuum applied during vacuum bagging forced powder into the intratow voids, Figs. 5c and 5d.

When the degree of impregnation of powder in the intertow pores was substantial, cracks

appeared during the drying process in the intertow regions, the cracks usually being parallel to the fabric layers, Fig. 5c. It is believed that these were caused by the shrinkage of the powder matrix within the large intertow pores as a result of drying, whilst the fiber architecture prevented the preform as a whole from shrinking. The effect was less pronounced when a larger particle size was used.

DEXA characterisation on the green preforms provided very clear, if qualitative, information on the powder distribution across the samples, Fig. 6a. When high solids content suspensions were used less uniformly impregnated samples resulted, presumably as a result of the higher viscosity of these suspensions, which made them more difficult to brush uniformly across the fabric discs. Similarly, when the finer powders were used the particles may be seen to be mainly located around the edges of the preforms whilst the reverse was true for the larger particle sizes. This may be due to the applied pressure squeezing the finer powders outwards towards the edge of the preforms during the compaction stage. These results suggest that a more uniform distribution of the initial precursor suspension across the fabric discs and the use of intermediate particle sizes, in the range 5 – 8 μm, are desirable to maximise the uniformity in the powder impregnation of the preforms.

Whilst the gas permeability results in Table II showed relatively little variation as a function of particle size or solid loading for the samples measured, they do show that the introduction of powder reduced the permeability significantly, from 16×10^{-12} m^2 for a powderless preform[11] to values of $1 – 2\times10^{-12}$ m^2. This suggests strongly that the powder blocks a significant fraction of the gas paths necessary for CVI. Subsequent work[3,8,9], however, demonstrated that all of the preforms could be successfully infiltrated by CVI.

Finally, it should be noted that whilst no mechanical test data was gathered for any of the

impregnated preforms produced in this work, those processed by VB were thinner, stronger, very handleable and less susceptible to delamination compared to the other methods. This is believed to result from the compression used under vacuum whilst the preform was still moist, the whole preform being strongly compacted.

(2) Electrophoretic infiltration

Vertical electrode: Due to settling of the powder in the suspension, it was not possible to achieve EPI successfully using vertical electrodes with powders coarser than 2.5 μm; the results obtained using the finer powders for suspension B are shown in Table III and Fig. 7. Irrespective of the particle sizes used, there was a clear trend as a function of the product of voltage and time, Fig. 7, with increased deposition being achieved at higher voltages and longer times as expected. However, for a given product of voltage × time the 0.6 μm particles resulted in greater powder deposition than the 2.5 μm particles (provided all layers within the tow were impregnated), which in turn led to greater porosity reduction, Table III. In addition, the powder deposition rate decreased as processing time increased, compare for example, E/5/25-100/30 and E/5/25-100/60 in Table III. This is also not surprising since the deposition rate is affected by the particle concentration in the suspension. This will decrease as deposition progresses, especially when the initial solids loading is low and the suspension is not stirred. Although the effect of stirring was briefly investigated, it was found that the gain in mass was reduced indicating that the movement of particles in the electric field was perturbed.

SEM examination revealed that both sizes of powder deposited on the front surface of each fabric layer forming a continuous film covering the exposed surface, with very little SiC powder penetration within the fiber tows, Fig. 8a and 8b. As expected, the 0.6 μm particles penetrated a little further than the 2.5 μm particles, however higher voltages resulted in less penetration.

Although this is perhaps counter-intuitive, higher voltages will have resulted in the particles accumulating on the fabric surface more rapidly, consequently blocking the paths into the intratow porosity. Nevertheless, the powders were deposited with a high density in the intertow porosity, Fig. 8c, leaving relatively few unimpregnated regions after stacking the fabric layers to form the preforms, Fig. 8a. Despite this, the impregnated preforms were very weak and suffered delamination very easily, preventing gas permeabilities being measured.

DEXA characterisation showed that the powder tended to form a 'crown' pattern around the centre, leaving the centre less impregnated than the periphery, Fig. 6b (the lack of deposition around the circumference arises from the presence of the polypropylene mask used to keep the fabric layer attached to the electrode). It is believed that this was caused by the lack of stirring during deposition resulting in sedimentation and hence preferential deposition at the bottom of each fabric layer attached to the electrode. Once randomly stacked up together, the 'crown' pattern was formed.

Rotating electrode: Since stirring the slurry reduced mass deposition by disturbing the motion of the particles within the suspension, a rotating electrode approach was investigated to improve the uniformity of the powder distribution across the fabric area. Whilst very little variation in the mass of powder deposited was observed in the range 0 to 6 rpm, a rotation of 3 rpm was found to be the optimum speed based on the uniformity of the powder deposition. This electrode proved to be more tolerant of stirring of the suspension and very low stirring speeds were found to benefit the uniformity of deposition on the fabric surface without significantly affecting the amount of powder deposited.

Horizontal electrode: The horizontal electrode arrangement enabled larger SiC particles to be deposited, indeed they benefited the process by adding a degree of gravitational settling and so,

as expected, the masses deposited were slightly more than for the vertical electrode, Fig. 9. They also resulted in less intratow penetration whilst continuing to achieve successful filling of the intertow porosity. The most even distributions across the fabric surface were observed to occur for deposition times of less than 90 s.

When the horizontal electrode was used without the application of an electric field, i.e. pure gravitational settling (GS), the mass of powder deposited was approximately halved but the distribution of powder across the fabric surface was slightly more even and the intertow macrovoids were efficiently filled, irrespective of the slurry used. This is presumably because the slower deposition rate yielded a more uniform build up of powder.

Throughout the work using EPI, the ethanol-based slurry B took less time to dry, but resulted in a greater degree of cracking and delamination of the preforms than the aqueous-based slurry C, presumably because of the faster rate of solvent movement.

(3) Combined processes

Table IV summarises the results obtained when powder was deposited on the fabric layers from slurry C by EPI, using the horizontal electrode arrangement and 50 V for 60 s, and then the resulting preforms were consolidated by VB. Very uniform powder deposition across the fabric layers was observed, Fig. 6c, with the intertow porosity densely filled but almost no penetration of the particles into the intratow porosity when the 6.7 and 10 μm SiC particle sizes were used, Fig. 10. The major advantage observed for this technique was the ability to produce relatively strong and well compacted preforms from the VB stage of the process, with high densities as a result of the EPI process, but without the SiC particles filling the intratow voids when the coarser SiC particles were used. Despite the higher densities, the gas permeabilities were a factor of 3 – 6 higher than for the VB route on its own supporting the view that the intratow gas channels, so

important for CVI, had not become blocked.

Table IV also shows the results obtained when gravitational settling of the SiC particles was used to coat the fabric layers using the horizontal electrode but without any electric field and then the preforms were consolidated using the VB process. Once again, the powder distribution across the preform diameter was uniform, the intertow porosity was densely filled and the intratow porosity remained largely empty. Although the gas permeability was similar for the combined EPI/VB process for the aqueous slurry C, when the ethanol-based slurry B was used the value was approximately doubled to almost that of the unimpregnated preforms.

IV Conclusions

Both the VB and EPI processes led to the impregnation of SiC fabric preforms with SiC powders, although the distribution of the powder was significantly different in the two cases, affecting both the strength and gas permeability of the final preforms. With the VB process, the SiC powder was forced into the intratow porosity and only filled the intertow porosity if the solids content of the suspension was sufficiently high; the opposite of what was required. In addition, the process relied on the manual brushing of the suspension onto the fabric disks; a process that led to a degree of variability despite attempts to control it. Much more uniform, controllable and reproducible deposition was achieved with the EPI process, with the intertow porosity being filled particularly densely but relatively little penetration of the particles into the intratow porosity, particularly when larger SiC particles were used. To avoid non-uniform distribution of the particles across the SiC fabric layers, a horizontal electrode arrangement was developed. This actually yielded slightly superior preforms when the electric field was turned off and gravity alone used to achieve deposition, although the time required obviously increased.

The main problem with the EPI process was that the resulting preforms were particularly weak

and delaminated easily during handling. In contrast, the VB-formed preforms were relatively strong. The combination of EPI using a horizontal electrode, with or without the electric field switched on, followed by VB yielded strong preforms with a high degree of powder loading but which also retained a high level of gas permeability, a major requirement for the subsequent CVI stage.

Acknowledgements

The authors would like to acknowledge funding by QinetiQ Ltd (formerly the Defence Evaluation Research Agency (DERA) of the UK).

References

1. T. M. Besmann, B. W. Sheldon, R. A. Lowden and D. P. Stinton, "Vapor-phase fabrication and properties of continuous-filament ceramic composites", *Science* **253** 1104-1109 (1991).
2. R. Naslain, "Design, preparation and properties of non-oxide CMCs for application in engines and nuclear reactors: an overview", *Comp. Sci. and Techn.* **64** 155-170 (2004).
3. D. Brewer, "HSR/EPM combustor materials development program", *Mater. Sci. Eng.* **A261** 284-291 (1999).
4. K. J. Probst., T. M. Besmann., D. P. Stinton, R. A. Lowden, T. J. Anderson and T.L. Starr, "Recent advances in forced-flow, thermal-gradient CVI for refractory composites", *Surfaces and Coatings Techn.* **120-121** 250-258 (1999).
5. B.W.Sheldon, "The control of gas phase kinetics to maximize densification during chemical vapour infiltration", *J. Mater. Res.* **5** [11] 2729-2736 (1990).
6. S. Bertrand., J. F. Lavaud, R. El Hadi, G. Vignoles and R. Pailler, "The thermal gradient-pulse flow CVI process: a new chemical vapour infiltration technique for the densification of fibre preforms", *J. Eur. Ceram. Soc.* **18** 857-870 (1998).
7. J.H. Kinney, T.M. Breunig, T.L. Starr, D. Haupt, M.C. Nichols, S.R. Stock, M.D. Butts and R.A. Saroyan, "X-ray tomographic study of chemical vapour infiltration processing of ceramic composites", *Science* **260** 789-791 (1993).
8. J.Y. Ofori and S.V. Sotirchos, "Dynamic convection-driven thermal gradient chemical vapour infiltration", *J. Mater. Res.* **11** [10] 2541-2555 (1996).
9. D. J. Skamser, J. J. Thomas, H.M. Jennings and D.L. Johnson, "Microwave heating of a changing material", *Ceram. Trans.* **59** 289-298 (1995).
10. A. Ortona, A. Donato, G. Filacchioni, U. De Angelis, A. La Barbera, C. A. Nannetti, B. Riccardi and J. Yeatman, "SiC-SiC$_f$ CMC manufacturing by hybrid CVI-PIP techniques:

process optimisation", *Fusion Eng. and Design* **51-52** 159-163 (2000).

11. D. Jaglin, J. Binner, B. Vaidhyanathan, C. Prentice, R.A. Shatwell and D.G. Grant, "Microwave heated chemical vapour infiltration: Densification mechanism of SiC_f/SiC Composites", *J. Am. Ceram. Soc.* **89** [9] 2710-2717 (2006).
12. R.J. Shinavski and R.J. Diefendorf, "CVI processing of thin C/HfB_2 composites", *Ceram. Eng. Sci. Proc.* **14** [9/10] 824-831 (1993).
13. M. Jones and T.L. Starr, "Enhancements to the Georgia Tech. chemical vapour infiltration process model for ceramic matrix composites", *Ceram. Eng. Sci. Proc.* **16** [5] 829-836 (1995).
14. W.J. Lackey, S. Vaidyaraman, G.B. Freeman and P.K. Agrawal, "Technique for monitoring densification during chemical vapour infiltration", *J. Am. Ceram. Soc.* **78** [4] 1131-1133 (1995).
15. T. Yano, K. Budiyanto, K. Yoshida and T. Iseki, "Fabrication of silicon carbide fiber-reinforced silicon carbide composite by hot-pressing", *Fusion Eng. and Design* **41** 157-163 (1998).
16. A. Sayano, C. Sutoh, S. Suyama, Y. Itoh and S. Nakagawa, "Development of a reaction-sintered silicon carbide matrix composite", *J. Nucl. Mater.* **271-272** 467-471 (1999).
17. J. J. Brennan, "Interfacial characterization of a slurry-cast melt-infiltrated SiC/SiC ceramic-matrix composite", *Acta Mater.* **48** 4619-4628 (2000).
18. D. Brewer, "HSR/EPM combustor materials development program", *Mater. Sci. Eng.* **A261** 284291 (1999).
19. H. O. Davies and D. R. Petrak, "Ceramic matrix composites using polymer pyrolysis and liquid densification processing", *J. Nucl. Mater.* **219** 26-30 (1995).

20. J. Gotoh, K. Tsugeki, A. Sakai and H. Nakayama, “Fabrication and mechanical properties of ceramic matrix composites by polymer impregnation and pyrolysis method”, *Proc. 4th Japan Int. SAMPE Symp.* pp. 240-245 (1995).

21. M.F. Gonon and S. Hampshire, “Comparison of two processes for manufacturing ceramic matrix composites from organometallic precursors”, *J. Eur. Ceram. Soc.* **19** 285-291 (1999).

22. Y-W. Kim, J-S. Song, S-W. Park and J-G. Lee, “Nicalon-fibre-reinforced silicon-carbide composites via polymer solution infiltration and chemical vapour infiltration”, *J. Mater. Sci.* **28** 3866-3868, (1993.)

23. S. Casadio, A. Donato, C.A. Nannetti, A. Ortona and M. Rescio, “Liquid infiltration and pyrolysis of SiC matrix composite materials”, *Ceram. Trans.* **58** 193-198 (1995).

24. S. M. Dong, Y. Katoh, A. Kohyama, S. T. Schwab and L. L. Snead, “Microstructural evolution and mechanical performances of SiC/SiC composites by polymer impregnation/microwave pyrolysis (PIMP) process”, *Ceram. Int.* **28** 899-905 (2002).

25. G. Ziegler, I. Ritcher and D. Suttor, “Fiber-reinforced composites with polymer-derived matrix: processing matrix formation and properties”, *Composites: Part A* **30** 411-417 (1999).

26. G.R. Sherwin, “Non-autoclave processing of advanced composite repairs”, *Int. J. of Adhesion & Adhesives* **19** 155-159 (1999).

27. G. Sala, “Advances in elastomeric tooling technology”, *Materials & Design* **17** [1] 33-42 (1996).

28. M.Z. Berbon, D.R. Dietrich, D.B. Marshall and D.P.H. Hasselman, “Transverse thermal conductivity of thin C/SiC composites fabricated by slurry infiltration and pyrolysis”, *J. Am. Ceram. Soc.* **84** [10] 2229-2234 (2001).

29. A. Timms, W. Westby, C. Prentice, D. Jaglin, R. A. Shatwell and J. G. Binner, “Reducing chemical vapour infiltration time for ceramic matrix composites”, *J. Microsc.*, **201-202** 316-

323 (2001).

30. P. Sarkar, S. Datta and P.S. Nicholson, “Functionally graded ceramic/ceramic and metal/ceramic composites by electrophoretic deposition”, *Composites Part B* **28B** 49-56 (1997).

31. S.N. Heavens, “Electrophoretic deposition as a processing route for ceramics”, *Advanced Ceramic Processing & Technology Vol. I*, pp. 255-283, Ed. J.G.P. Binner, Noyes Publications (1990).

32. A.R. Boccaccini, I. MacLaren and M.H. Lewis, “Electrophoretic deposition infiltration of 2-D woven SiC fibre mats with mixed sols of mullite composition”, *J. Eur. Ceram. Soc.* **17** 1545-1550 (1997).

33. A. Borner and R. Herbig, “ESA measurement for electrophoretic deposition of ceramic materials”, *Colloids and Surfaces A: Physicochemical and Engineering Aspects* **159** 439-447 (1999).

34. H.H. Streckert and J.D. Katz, “Microwave densification of electrophoretically infiltrated silicon carbide composite”, *J. Mater. Sci.* **32** 6429-6433 (1997).

35. S. Kooner, J.J. Campaniello S., Pickering and E. Bullock, “Fiber reinforced ceramic matrix composite fabrication by electrophoretic infiltration”, *Ceram. Trans.* **58** 155-160 (1995).

36. D. Jaglin, J. Binner, C. Prentice, R. Shatwell, L. Timms and W. Westby, “SiC_f/SiC fabrication via vacuum bagging, electrophoretic infiltration and microwave enhanced CVI”, 9th Eur. Conf. on Composite Materials (ECCM 9) proceedings CD, Institute of Materials, Minerals and Mining, UK (2000).

37. A. P. Philipse, “Non-darcian airflow through ceramic foams”, *J. Am. Ceram. Soc.*, **74** [4] 728-732 (1991).

38. T. L. Starr and N. Hablutzel, ‘‘Measurement of gas transport through fiber preforms and densified composites for chemical vapour infiltration,’’ *J. Am. Ceram. Soc.* **81** [5] 1298–304 (1998).

39. J. Binner, B. Vaidhyanathan and D. Jaglin, “Microwave heated chemical vapour infiltration of SiC powder impregnated SiC fibre preforms”, Advances in Applied Ceramics: Structural, Functional and Bioceramics, *In Press*.

Captions

Fig. 1: SEM images of SiC_f/SiC composites processed by CVI (a) low magnification showing large intertow voids and (b) high magnification showing fine intratow porosity. 72 x 72 dpi

Fig. 2: Schematic diagrams showing (a) the vacuum bagging equipment and (b) the electrophoretic impregnation system. 72 x 72 dpi

Fig. 3: Design variations for the anode used for EPI of SiC powder from suspension onto SiC fabric layers. 72 x 72 dpi

Fig. 4a: Reduction in porosity observed in the VB preforms as a function of the solids loading in the SiC slurries. 72 x 72 dpi

Fig. 4b: Reduction in porosity observed in the VB preforms as a function of the particle size in the SiC slurries. 72 x 72 dpi

Fig. 5: SEM cross sectional micrographs of preforms prepared by VB at two different magnifications (a) and (c) V/30/6, (b) and (d) V/20/6. 72 x 72 dpi

Fig. 6: Colour enhanced ~~ERA~~ DEXA scans for samples prepared by a) VB, b) EPI using the vertical electrode and c) combined VB and EPI using the horizontal electrode. 72 x 72 dpi

Fig. 7: Reduction in porosity versus (voltage×time) applied during the EPI process using the vertical electrode. 72 x 72 dpi

Fig. 8: Low and high magnification SEM images of cross sections of preforms formed by EPI (a) and (b) E/5/6-50/90† and (c) E/5/6-100/45. 72 x 72 dpi

Fig. 9: Reduction in porosity versus deposition time for EPI using the vertical (V) and horizontal (H) electrodes and different SiC particle sizes. 72 x 72 dpi

Fig. 10: Low and high magnification SEM images of cross sections of preforms formed by combined VB and EPI (a) and (b) EV/5/25-50/60; (c) and (d) EV/5/67-50/60 and (e) and (f) EV/5/100-50/60. 72 x 72 dpi

Table I: Mean particle size and source of SiC particles used.

Table II: Impregnation results achieved by the VB process.

Table III: Impregnation results achieved by the EPI process.

Table IV: Impregnation results achieved by the combined horizontal EPI and VB processes and the combined horizontal GS and VB processes.

Table I**:** Mean particle size and source of SiC particles used.

Mean particle size / μm	Source
0.6	UF15, HC Starck, Goslar, Germany
2.5	ESK1500F, ESK, Kempten, Germany
6.7	Reliable Techniques, Newcastle-under-Lyme, UK
10.0	Carborex BW Micro F 600 PV, Washington Mills Electro Minerals, Manchester, UK
12.8	Silkaride CS F1200, Washington Mills Electro Minerals, Manchester, UK

Table II: Impregnation results achieved by the VB process.

Sample	Slurry type	Solid loading / %	Particle size / μm	V_f / %	V_p / %	V.R. / %	Relative density / %	Gas permeability[#] / 10^{-12} m^2
V/20/6	A	20	0.6	25	9	12	34	*
V/20/25	A	20	2.5	23	6	10	29	*
V/20/128	A	20	12.8	21	8	11	29	*
V/30/6	A	30	0.6	35	15	23	50	*
V/30/100	A	30	10.0	14	15	17	29	1.3
V/35/6	A	35	0.6	21	18	23	39	2.0
V/35/25	A	35	2.5	19	16	28	35	1.9
V/35/67	A	35	6.7	16	19	23	35	1.8
V/35/100	A	35	10.0	18	21	26	39	1.1
V/40/100	A	40	10.0	16	21	25	37	1.0

[#]16×10^{-12} m^2 for a powderless preform
*Technique not available at the time

Table III: Impregnation results achieved by the EPI process.

Sample	Slurry type	Solid loading / %	Particle size / μm	Electrode type	Voltage / V	Time / s	V_f / %	V_p / %	~~Void reduction~~ V.R. / %	Relative density / %
E/5/6-50/45†	B	5	0.6	Vertical	50	45	21	7	9	28
E/5/6-50/60	B	5	0.6	Vertical	50	60	17	15	18	32
E/5/6-50/90	B	5	0.6	Vertical	50	90	16	18	21	34
E/5/6-50/90†	B	5	0.6	Vertical	50	90	22	12	15	34
E/5/6-100/45	B	5	0.6	Vertical	100	45	20	19	24	39
E/5/25-50/60	B	5	2.5	Vertical	50	60	20	11	14	31
E/5/25-100/30	B	5	2.5	Vertical	100	30	22	13	17	35
E/5/25-100/60	B	5	2.5	Vertical	100	60	19	21	26	40
E/10/25-50/60	B	10	2.5	Vertical	50	60	18	26	32	44
E/5/25-50/60	B	5	2.5	Horizontal	50	60	18	12	15	30

† Alternate layers impregnated

Table IV: Impregnation results achieved by the combined horizontal EPI and VB processes and the combined horizontal GS and VB processes.

Sample	Slurry type	Solid loading / %	Particle size / μm	V_f / %	V_p / %	~~Void reduction~~ V.R. / %	Relative density / %	Gas permeability / 10^{-12} m^2
EV/5/25-50/60	C	5	2.5	18	17	21	35	6.9
EV/5/67-50/60	C	5	6.7	21	18	23	39	6.8
EV/5/100-50/60	C	5	10	21	19	24	40	6.3
GV/5/67-B	B	5	6.7	17	19	23	36	12.8
GV/5/67-C	C	5	6.7	19	22	27	41	6.8
GV/5/100-B	B	5	10	21	20	25	41	10.6
GV/5/100-C	C	5	10	20	20	25	40	6.0

Use of Electrophoretic Impregnation and Vacuum Bagging to Impregnate SiC powder into SiC Fiber Preforms

Jon Binner*, Bala Vaidhyanathan, David Jaglin and Sarah Needham†

Department of Materials, Loughborough University, Loughborough, Leicestershire LE11 3TU, United Kingdom

Abstract

Techniques based on vacuum bagging (VB) and electrophoretic impregnation (EPI) have been investigated for the impregnation of SiC powder into layered Nicalon SiC fabric preforms. The aim was to produce pre-impregnated samples for subsequent chemical vapour infiltration (CVI) with reduced intertow porosity that arises from the construction of the fabric layers whilst leaving unblocked the intratow porosity that is so indispensable for a successful infiltration. Since the goal was simply to learn about the ability to impregnate the samples, no interphase coating was applied to the fibers as would normally be used when producing SiC_f-SiC composites. Whilst the VB process generally yielded much stronger preforms, depending on the pressure used and the powder particle size, it resulted in powder becoming located in the intratow rather than the intertow porosity. In contrast, provided an appropriate electrode arrangement was used, EPI offered the potential for a more controlled impregnation process with the powder primarily found in the intertow porosity; however, the preforms were very weak and delaminated easily. The combination of the two processes resulted in a very successful approach, with greater uniformity of particle infiltration and higher green strengths, whilst largely avoiding impregnating the intratow porosity.

* J.binner@Lboro.ac.uk
† Now with Rolls Royce plc., UK

I Introduction

SiC_f/SiC composites are very promising materials for high temperature structural applications because of their good thermal stability and excellent mechanical properties. Of the various techniques used to produce fiber reinforced ceramic matrix composites, chemical vapour infiltration (CVI) has received considerable attention[1-2]. Combining isothermal or temperature gradient, isobaric or pressure gradient features, as well as the use of pulsing, CVI results in composites still containing 10 - 20% residual porosity[3-6] however. This is mainly due to two reasons: (i) when the minimum percolation threshold for transport through the pore structure is reached, infiltration becomes more and more difficult as the pore size decreases resulting in deposition occurring on the outside of the fiber network, and (ii) when the composite reaches a fractional density of ~70% the surface area becomes dominated by the macropores; these can take too long to infiltrate from a commercial viewpoint. It is the last 30% of densification that is financially costly because the infiltration time becomes extended (to days and even weeks in some cases) during this phase[7] and to produce fiber-reinforced ceramic matrix composites (FRCMCs) by any form of CVI at a commercially acceptable cost, the processing time must be kept short[8].

As implied above, the porosity itself can be divided into two main types; fine intratow and much larger intertow porosity. In fibrous preforms densified up to 82% of theoretical[9], the lamination of the plies combined with the weave design can result in intertow pores being as large as 0.3 to 0.6 mm in width and tens of millimetres long. There is also the problem of the packing of the fabric layer in the Z-direction[10]. Fig. 1a[11] provides an illustration of this type of porosity, which is the most harmful type of defect for mechanical properties as well as providing a path for corrosive agents. When present, these pores are very difficult to eliminate in fiber preforms produced from the lay-up of fiber sheets. In contrast, intratow pores are typically <15 μm in diameter and are formed when the matrix deposition on the individual fibers traps small pores,

Fig. 1b. Whilst some will probably always be residual after CVI-based processes, they are not considered to be particularly detrimental to the overall strength of the composite due to their small size[9]. Nevertheless, the elimination of this porosity by the use of the right infiltration conditions would also undoubtedly be desirable – provided it can be achieved without a significant increase in processing time and hence costs.

Two-stage CVI processes have therefore been investigated where, under the right conditions, the initial stage sees the efficient filling of the finer, intratow porosity and the second stage seeks to fill as much of the coarser, intertow pores as possible within the economic limitations of the process[12-13]. For example, using marker layers, Lackey *et al.*[14] found that when using forced-flow CVI, intratow infiltration could be virtually complete within the first 2 h, although filling the intertow porosity took considerably longer. One potential problem with this approach is that some intertow porosity can become trapped in the structure when the intratow porosity becomes filled.

Although not the focus of this paper, many other techniques are available for the fabrication of FRCMCs as well as CVI. For example, hot-pressing techniques have been used[15] in which the stacked green body was hot-pressed at up to 2023 K with a matrix consisting of β-SiC powder and sintering aids. Unfortunately, the composite displayed brittle behaviour even though Hi-Nicalon fibers were used. An approach based on slurry-cast melt infiltration with reaction-sintering[16-18] used a slurry consisting of SiC powder or a mixture of SiC powder and carbon powder in water that was impregnated into the SiC fiber preform. The green composite was then reaction sintered at 1720 K with melted silicon to obtain a rich SiC matrix. Disadvantages lay in the need for a designed mould and residual silicon metal as high as 15-20 vol.%, despite the low porosity achieved.

An alternative approach can be based on the pre-impregnation of the macropores by a process

other than CVI and polymer impregnation and pyrolysis (PIP) processes are very common and effective manufacturing techniques for high performance SiC_f/SiC composites[19-24]. Six or more cycles of impregnations, followed by the pyrolysis, are typically required to achieve densities of 80-85%. An important aspect of the process is that the matrix development affects the mechanical properties by inducing residual stresses due to shrinkage of the matrix during pyrolysis and also the anisotropy of the thermal expansion coefficient between the fibers and matrix[25].

The introduction of powder into the PIP was investigated by Gonon and Hampshire[21] who used polysilazane as precursor with the addition of Si_3N_4 powder into SiC fiber preforms; 7 to 8 cycles of precursor impregnation and pyrolysis were required to reduce the porosity to approximately 15%, but the presence of powder did not allow good cross-linking of the precursor and resulted in lower mechanical properties than the composite with the polymer alone, a result confirmed by Casadio[23]. Gotoh *et al.*[20] also pointed out that optimisation of the mechanical properties relies on the right volume of fiber and sintering aids. Fast heating techniques such as microwaves can be applied during the pyrolysis stage, providing time and energy savings since suitably high temperatures can be induced in a matter of minutes. Dong and co-authors[24] used this particular technique but required 8 cycles of impregnation to achieve a final density of 78%.

Combining PIP with CVI allowed Kim *et al.*[22] to achieve an initial preform density of up to 70% after PIP, the subsequent isobaric, isothermal CVI step yielding a composite density of 82%. Ortona *et al.*[10] found that an initial CVI stage can prevent the swelling of the preform during the PIP stages.

Two simple and rapid processes that have been shown to lead to a successful pre-impregnation in other, non-SiC fiber-based systems are vacuum bagging (VB) and electrophoretic

impregnation (EPI). VB is a relatively simple process that was developed by Rolls Royce in the 1980s for the preparation and/or repair of polymer matrix carbon fiber composites in the aerospace industry[26-28]. This technique has subsequently been modified for the impregnation of ceramic powders between tows and layers of fiber-based fabrics in order to reduce the porosity and improve the green strength[29]. The fabric layers are individually coated with ceramic slurry and stacked, prior to being dried and consolidated under vacuum. Process parameters are mainly associated with the preparation of the slurry, which controls the particle size being used and the amount of powder to be impregnated, and the pressure involved during vacuum bagging.

EPI is directly related the electrophoretic deposition process (EPD) wherein charged particles are deposited on an electrode surface via their migration under the action of an electrical field[30]. In the EPI process, a fiber preform is impregnated via the deposition of particles from a slurry onto individual cloth layers prior to assembly into the preform. The movement of ceramic particles in a suspension within an electric field is governed mainly by factors such as the field strength[31], the pH of the suspension and its ionic strength[32]. The amount of polyelectrolyte addition also influences the rate of deposition and the homogeneity of the deposited material[33]. Green composite microstructures with good infiltration uniformity and few macro defects have been obtained by this technique[34-35] and previous work with a SiC_f/SiC system resulted an increase in density from 20 vol.% (the initial fiber preform density) to over 40 vol.% in only 20 minutes[36].

In the present work, a methodical examination of the use of stand-alone VB and EPI techniques as well as their combination with a number of geometrical modifications has been undertaken with a view to producing SiC powder-loaded SiC fiber preforms that are suitable for subsequent infiltration with a SiC matrix using CVI. The goal was to fill the larger intertow pores, so reducing

the time that would be needed during a subsequent CVI stage, whilst avoiding the introduction of powder particles within the tows themselves. The particles can cause abrasion during use and damage the tows. In addition, it was desired to produce impregnated fiber preforms that were mechanically robust and capable of being handled prior to and during the CVI stage.

II Experimental procedure

(1) Materials

The preforms were made from NL-202 SiC fibers (Nippon Carbon, Tokyo, Japan) woven (by Sigmatex Ltd., UK) into a 2D plain weave NP1616 pattern. Forty eight mm circular discs were cut from the cloth using a metal template and ceramic scissors. The sizing agent was removed by heating the fiber discs in a furnace at 600°C for 2 h. Note, no attempt was made in this work to apply an interphase coating to the fibers prior to undertaking the impregnation with powder particles. This was because it was not believed that such a coating would materially affect the identification of the best choice of impregnation process, which was the goal of this work. For the impregnation experiments themselves, five SiC powders with mean particle sizes of approximately 0.6, 2.5, 6.7, 10.0 and 12.8 μm were used; their details are provided in table 1.

(2) SiC powder slurry preparation

Three types of slurries were prepared. Slurry A was used during the impregnation of preforms by vacuum bagging (VB), whilst slurries B and C were used for electrophoretic impregnation (EPI) and gravitational settling (GS).

Slurry A: Aqueous slurries containing solids loadings between 20 and 40 vol.% were prepared for all five of the SiC powders. The powders were dispersed using 1 to 1.5 wt.% of Glascol K11 (Ciba Speciality Chemicals, Bradford, UK) and the pH was fixed at 9.0 ± 0.2 via the addition of ammonia solution. To eliminate powder agglomerates, the slurries were ball-milled in airtight

polyethylene bottles using zirconia media for 24 h, the viscosity being regularly monitored. Note that, although slurries with a solid loading higher than 45 vol.%, were prepared, problems were experienced with subsequent wetting of the fiber fabric and hence these slurries were discarded.

Slurry B: Ethanol-based slurries containing solids loadings of 5 and 10 vol.% were prepared for four of the SiC powders, the powders being dispersed using 0.5 vol.% of triethylamine (Ciba Speciality Chemicals, Bradford, UK); the pH was 9.0 ± 0.2. The 12.8 μm SiC powder was not used as it was found that particle migration was difficult to achieve at the voltages used. To remove powder agglomerates, during preparation the slurries were exposed to ultrasonic energy at 23 kHz (Soniprep 150 Ultrasonicator, MSE Scientific Instruments, Manchester, UK) for a minimum of 60 s together with mechanical agitation using a magnetic stirrer.

Slurry C: An identical preparation route as for slurry B was used to prepare aqueous suspensions containing 5 vol.% of SiC powders for all five of the SiC powders, again with the addition of ~0.5 vol.% of triethylamine. The pH was again 9.0 ± 0.2. Ultrasonic energy and mechanical agitation was again used, as described for slurry B.

(3) Vacuum bagging

A small amount of slurry A was applied to the discs of SiC fabric using a nylon brush. Since the impregnation of the powder was performed manually, the VB technique potentially lacked repeatability with respect to the amount of powder deposited on each fabric layer. To minimise this problem each layer was weighed after brushing to ensure that a consistent amount had been deposited. Ten discs were then stacked and the layers compressed using a roller. Each preform was placed in the vacuum bagging equipment (Townsend & Mercer Ltd., Croydon, UK), Fig. 2a, and dried overnight at temperatures ranging from 20 to 60°C, a rotary pump being used to apply a vacuum of ~0.5×10^5 Pa. The combination of the pressure used and drying process meant that the stack of disks held together sufficiently for subsequent handling.

(4) Electrophoretic impregnation and gravitational settling

Fig. 2b is a schematic diagram of the experimental arrangement used for the electrophoretic impregnation process. Initially, flat stainless steel plates were used as electrodes, Fig. 3a, placed vertically in the suspension 15 mm apart. The fiber preforms were attached to the anode since gas formed at the cathode that could have become trapped in the green compact. Two further electrode systems were devised following the initial results with the vertical electrodes, these being (i) vertical electrodes accommodating a rotating device for the anode, Fig. 3b, with speeds from 0 to 6 rpm and (ii) horizontal electrodes, Fig. 3c. The latter were also used without an electric field for comparative work involving the gravitational settling (GS) of particles. The authors are not aware of any previous work in terms of impregnating fiber preforms using simple gravitational settling; it was used simply to get a feel for how important the electrical field was.

For each impregnation a fabric disc measuring 48 mm diameter was laid on top of the appropriate anode and a polypropylene (PP) mask the same size as the electrode clamped over it using plastic grips. The PP cover had a 40 mm internal diameter opening cut in it to allow impregnation to occur into the preform; it should be noted that this design prevented any deposition of SiC powder in the outer 4 mm of the preform. Electrophoretic impregnations were carried out by applying a potential difference ranging from 50 to 100 V in constant voltage mode using slurries B and C. Each fabric disc was processed and the anode wiped clean of slurry before the next disc was attached on top of the previous, wet disc. The whole process was performed as fast as possible and the stack of ten powder impregnated discs was then allowed to dry overnight at room temperature. For all of the EPI-based processes, the final drying stage provided some strength to the stack of disks but they needed very careful handling.

For the gravitational settling (GS) process, the horizontal anode was used with no applied field. Each fabric disc was mounted on the anode as for the EPI process and held in place by the PP

cover. The slurry was stirred and, the moment the stirring stopped, the anode was plunged to the bottom of the beaker containing the suspension for a set period of time. The anode was then removed from the beaker and a fresh fabric disc placed in position on top of the wet one and the process repeated until a preform consisting of ten discs had been produced. Once again, the stack of discs produced needed very careful handling to prevent them delaminating.

(5) Combined process

Fabric discs were initially infiltrated with slurries B and C using the EPI and GS processes and then subsequently consolidated using the VB process as described previously. The use of the latter provided adequate strength to the stack for subsequent handling.

(6) Characterisation

Specimen diameters and thicknesses were measured using a vernier calliper gauge. The relative fiber volume, V_f, and relative powder volume, V_p, of the preforms (as a percentage of the total preform volume) were determined from the mass of the preform prior to powder impregnation, m_f, and its mass after powder impregnation, m_s, (from which the mass of powder impregnated, m_p, could be calculated) and the actual volume of the preforms, V_s, the latter being calculated from its geometry:

$$V_f = \frac{m_f}{V_s \rho_f} \times 100\ (\%) \qquad \textbf{(1)}$$

$$V_p = \frac{(m_s - m_f)}{V_s \ \rho_{\mathrm{SiC}}} = \frac{m_p}{V_s \ \rho_{\mathrm{SiC}}} \times 100\ (\%) \qquad \textbf{(2)}$$

where ρ_f is the density of NL-202 Nicalon fiber (2.55 g cm^{-3}) and ρ_{SiC} is the density of stoichiometric SiC (3.21 g cm^{-3}).

Assessment of the efficiency of the different processes was achieved by calculating the void reduction:

$$V.R. = (1 - \frac{100 - (V_f + V_p)}{100 - V_f}) \times 100 \ (\%) \quad \textbf{(3)}$$

Scanning electron microscopy was used to study both the powder distribution across the sample and the level of impregnation into the intratow and intertow porosity. The use of secondary and backscattered electron imaging allowed the powder additions to be differentiated with clarity from the fibers.

Dual energy X-ray absorptiometry (DEXA) also provided information on the powder distribution after impregnation. A Lunar DPX-L DEXA was calibrated for SiC materials[11] and photon attenuation maps acquired which, particularly when artificially coloured, provided a clear, qualitative representation of density variations across the diameter of the specimens.

Using Darcy's law for laminar viscous flow in porous materials[37], the gas permeability of the samples, *K,* was calculated by plotting the ratio of the pressure difference across the sample thickness against the airflow. This provided a rough measure of the permeability of the preforms, with a view to ensuring that a subsequent CVI process would be capable of occurring. The pressure drop, ΔP, across the preforms (thickness L) was measured from the difference between the inlet and outlet pressure in a permeability rig similar to that described elsewhere[38]. The viscosity of the air was taken as $\mu_{air} = 1.827 \times 10^{-5}$ Pa s.

III Results & Discussion

As indicated above, the primary aim of the impregnation experiments was to reduce the intertow pore sizes of the preform, in order to shorten a subsequent chemical vapour infiltration process (not reported in this work), whilst ensuring that the preform has enough green strength to allow

handling and that the intratow porosity was accessible for infiltration. The distribution of the powder in the intertow and intratow porosity, as well as the uniformity of its distribution across the fiber preform, were therefore of key importance.

Throughout the results, including Tables II – IV, the samples are identified by a code in which the first letter(s) is indicative of the impregnation system used; V for vacuum bagging, E for electrophoretic impregnation, G for gravitational settling, EV for combined electrophoretic impregnation and vacuum bagging and GV for combined gravitational settling and vacuum bagging.

(1) Vacuum bagging

The vacuum bagging results are shown in Table II and Fig. 4. As expected, it can be seen that the amount of powder impregnated into the preforms (indicated by the values of V_p) was mainly influenced by the solids loading of the slurry, rather than the particle size. Repeatability of the results were confirmed with similar samples displaying V_p values (and hence V.R. and relative density values)within ±1% variation. SEM analysis revealed that compaction of the layers occurred with the intertow pores being reduced to typically 50-100 μm wide (the uncompacted intertow pores were up to ~500 μm wide). When the solids loading was ≥30 vol.% the particles systematically infiltrated these intertow voids leaving only a few, small regions unfilled, Fig. 5a. In contrast, when a 20% slurry was used very little intertow powder impregnation occurred, Fig. 5b, with just a little localised impregnation. For all solids contents, impregnation of the tows occurred for the 0.6 and 2.5 μm particle sizes as the pressure and vacuum applied during vacuum bagging forced powder into the intratow voids, Figs. 5c and 5d.

When the degree of impregnation of powder in the intertow pores was substantial, cracks appeared during the drying process in the intertow regions, the cracks usually being parallel to

the fabric layers, Fig. 5c. It is believed that these were caused by the shrinkage of the powder matrix within the large intertow pores as a result of drying, whilst the fiber architecture prevented the preform as a whole from shrinking. The effect was less pronounced when a larger particle size was used.

DEXA characterisation on the green preforms provided very clear, if qualitative, information on the powder distribution across the samples, Fig. 6a. When high solids content suspensions were used less uniformly impregnated samples resulted, presumably as a result of the higher viscosity of these suspensions, which made them more difficult to brush uniformly across the fabric discs. Similarly, when the finer powders were used the particles may be seen to be mainly located around the edges of the preforms whilst the reverse was true for the larger particle sizes. This may be due to the applied pressure squeezing the finer powders outwards towards the edge of the preforms during the compaction stage. These results suggest that a more uniform distribution of the initial precursor suspension across the fabric discs and the use of intermediate particle sizes, in the range 5 – 8 μm, are desirable to maximise the uniformity in the powder impregnation of the preforms.

Whilst the gas permeability results in Table II showed relatively little variation as a function of particle size or solid loading for the samples measured, they do show that the introduction of powder reduced the permeability significantly, from 16×10^{-12} m^2 for a powderless preform[11] to values of 1 – 2×10^{-12} m^2. This suggests strongly that the powder blocks a significant fraction of the gas paths necessary for CVI. Subsequent work[39], however, demonstrated that all of the preforms could be successfully infiltrated by CVI.

Finally, it should be noted that whilst no mechanical test data was gathered for any of the impregnated preforms produced in this work, those processed by VB were thinner, stronger,

very handleable and less susceptible to delamination compared to the other methods. This is believed to result from the compression used under vacuum whilst the preform was still moist, the whole preform being strongly compacted.

(2) Electrophoretic infiltration

Vertical electrode: Due to settling of the powder in the suspension, it was not possible to achieve EPI successfully using vertical electrodes with powders coarser than 2.5 μm; the results obtained using the finer powders for suspension B are shown in Table III and Fig. 7. Irrespective of the particle sizes used, there was a clear trend as a function of the product of voltage and time, Fig. 7, with increased deposition being achieved at higher voltages and longer times as expected. However, for a given product of voltage × time the 0.6 μm particles resulted in greater powder deposition than the 2.5 μm particles (provided all layers within the tow were impregnated), which in turn led to greater porosity reduction, Table III. In addition, the powder deposition rate decreased as processing time increased, compare for example, E/5/25-100/30 and E/5/25-100/60 in Table III. This is also not surprising since the deposition rate is affected by the particle concentration in the suspension. This will decrease as deposition progresses, especially when the initial solids loading is low and the suspension is not stirred. Although the effect of stirring was briefly investigated, it was found that the gain in mass was reduced indicating that the movement of particles in the electric field was perturbed.

SEM examination revealed that both sizes of powder deposited on the front surface of each fabric layer forming a continuous film covering the exposed surface, with very little SiC powder penetration within the fiber tows, Fig. 8a and 8b. As expected, the 0.6 μm particles penetrated a little further than the 2.5 μm particles, however higher voltages resulted in less penetration. Although this is perhaps counter-intuitive, higher voltages will have resulted in the particles

accumulating on the fabric surface more rapidly, consequently blocking the paths into the intratow porosity. Nevertheless, the powders were deposited with a high density in the intertow porosity, Fig. 8c, leaving relatively few unimpregnated regions after stacking the fabric layers to form the preforms, Fig. 8a. Despite this, the impregnated preforms were very weak and suffered delamination very easily, preventing gas permeabilities being measured.

DEXA characterisation showed that the powder tended to form a 'crown' pattern around the centre, leaving the centre less impregnated than the periphery, Fig. 6b (the lack of deposition around the circumference arises from the presence of the polypropylene mask used to keep the fabric layer attached to the electrode). It is believed that this was caused by the lack of stirring during deposition resulting in sedimentation and hence preferential deposition at the bottom of each fabric layer attached to the electrode. Once randomly stacked up together, the 'crown' pattern was formed.

Rotating electrode: Since stirring the slurry reduced mass deposition by disturbing the motion of the particles within the suspension, a rotating electrode approach was investigated to improve the uniformity of the powder distribution across the fabric area. Whilst very little variation in the mass of powder deposited was observed in the range 0 to 6 rpm, a rotation of 3 rpm was found to be the optimum speed based on the uniformity of the powder deposition. This electrode proved to be more tolerant of stirring of the suspension and very low stirring speeds were found to benefit the uniformity of deposition on the fabric surface without significantly affecting the amount of powder deposited.

Horizontal electrode: The horizontal electrode arrangement enabled larger SiC particles to be deposited, indeed they benefited the process by adding a degree of gravitational settling and so, as expected, the masses deposited were slightly more than for the vertical electrode, Fig. 9.

They also resulted in less intratow penetration whilst continuing to achieve successful filling of the intertow porosity. The most even distributions across the fabric surface were observed to occur for deposition times of less than 90 s.

When the horizontal electrode was used without the application of an electric field, i.e. pure gravitational settling (GS), the mass of powder deposited was approximately halved but the distribution of powder across the fabric surface was slightly more even and the intertow macrovoids were efficiently filled, irrespective of the slurry used. This is presumably because the slower deposition rate yielded a more uniform build up of powder.

Throughout the work using EPI, the ethanol-based slurry B took less time to dry, but resulted in a greater degree of cracking and delamination of the preforms than the aqueous-based slurry C, presumably because of the faster rate of solvent movement.

(3) Combined processes

Table IV summarises the results obtained when powder was deposited on the fabric layers from slurry C by EPI, using the horizontal electrode arrangement and 50 V for 60 s, and then the resulting preforms were consolidated by VB. Very uniform powder deposition across the fabric layers was observed, Fig. 6c, with the intertow porosity densely filled but almost no penetration of the particles into the intratow porosity when the 6.7 and 10 μm SiC particle sizes were used, Fig. 10. The major advantage observed for this technique was the ability to produce relatively strong and well compacted preforms from the VB stage of the process, with high densities as a result of the EPI process, but without the SiC particles filling the intratow voids when the coarser SiC particles were used. Despite the higher densities, the gas permeabilities were a factor of 3 – 6 higher than for the VB route on its own supporting the view that the intratow gas channels, so important for CVI, had not become blocked.

Table IV also shows the results obtained when gravitational settling of the SiC particles was used to coat the fabric layers using the horizontal electrode but without any electric field and then the preforms were consolidated using the VB process. Once again, the powder distribution across the preform diameter was uniform, the intertow porosity was densely filled and the intratow porosity remained largely empty. Although the gas permeability was similar for the combined EPI/VB process for the aqueous slurry C, when the ethanol-based slurry B was used the value was approximately doubled to almost that of the unimpregnated preforms.

IV Conclusions

Both the VB and EPI processes led to the impregnation of SiC fabric preforms with SiC powders, although the distribution of the powder was significantly different in the two cases, affecting both the strength and gas permeability of the final preforms. With the VB process, the SiC powder was forced into the intratow porosity and only filled the intertow porosity if the solids content of the suspension was sufficiently high; the opposite of what was required. In addition, the process relied on the manual brushing of the suspension onto the fabric disks; a process that led to a degree of variability despite attempts to control it. Much more uniform, controllable and reproducible deposition was achieved with the EPI process, with the intertow porosity being filled particularly densely but relatively little penetration of the particles into the intratow porosity, particularly when larger SiC particles were used. To avoid non-uniform distribution of the particles across the SiC fabric layers, a horizontal electrode arrangement was developed. This actually yielded slightly superior preforms when the electric field was turned off and gravity alone used to achieve deposition, although the time required obviously increased.

The main problem with the EPI process was that the resulting preforms were particularly weak and delaminated easily during handling. In contrast, the VB-formed preforms were relatively

strong. The combination of EPI using a horizontal electrode, with or without the electric field switched on, followed by VB yielded strong preforms with a high degree of powder loading but which also retained a high level of gas permeability, a major requirement for the subsequent CVI stage.

Acknowledgements

The authors would like to acknowledge funding by QinetiQ Ltd (formerly the Defence Evaluation Research Agency (DERA) of the UK).

References

1. T. M. Besmann, B. W. Sheldon, R. A. Lowden and D. P. Stinton, "Vapor-phase fabrication and properties of continuous-filament ceramic composites", *Science* **253** 1104-1109 (1991).
2. R. Naslain, "Design, preparation and properties of non-oxide CMCs for application in engines and nuclear reactors: an overview", *Comp. Sci. and Techn.* **64** 155-170 (2004).
3. D. Brewer, "HSR/EPM combustor materials development program", *Mater. Sci. Eng.* **A261** 284-291 (1999).
4. K. J. Probst., T. M. Besmann., D. P. Stinton, R. A. Lowden, T. J. Anderson and T.L. Starr, "Recent advances in forced-flow, thermal-gradient CVI for refractory composites", *Surfaces and Coatings Techn.* **120-121** 250-258 (1999).
5. B.W.Sheldon, "The control of gas phase kinetics to maximize densification during chemical vapour infiltration", *J. Mater. Res.* **5** [11] 2729-2736 (1990).
6. S. Bertrand., J. F. Lavaud, R. El Hadi, G. Vignoles and R. Pailler, "The thermal gradient-pulse flow CVI process: a new chemical vapour infiltration technique for the densification of fibre preforms", *J. Eur. Ceram. Soc.* **18** 857-870 (1998).
7. J.H. Kinney, T.M. Breunig, T.L. Starr, D. Haupt, M.C. Nichols, S.R. Stock, M.D. Butts and R.A. Saroyan, "X-ray tomographic study of chemical vapour infiltration processing of ceramic composites", *Science* **260** 789-791 (1993).
8. J.Y. Ofori and S.V. Sotirchos, "Dynamic convection-driven thermal gradient chemical vapour infiltration", *J. Mater. Res.* **11** [10] 2541-2555 (1996).
9. D. J. Skamser, J. J. Thomas, H.M. Jennings and D.L. Johnson, "Microwave heating of a changing material", *Ceram. Trans.* **59** 289-298 (1995).
10. A. Ortona, A. Donato, G. Filacchioni, U. De Angelis, A. La Barbera, C. A. Nannetti, B. Riccardi and J. Yeatman, "SiC-SiC$_f$ CMC manufacturing by hybrid CVI-PIP techniques:

process optimisation", *Fusion Eng. and Design* **51-52** 159-163 (2000).

11. D. Jaglin, J. Binner, B. Vaidhyanathan, C. Prentice, R.A. Shatwell and D.G. Grant, "Microwave heated chemical vapour infiltration: Densification mechanism of SiC_f/SiC Composites", *J. Am. Ceram. Soc.* **89** [9] 2710-2717 (2006).
12. R.J. Shinavski and R.J. Diefendorf, "CVI processing of thin C/HfB_2 composites", *Ceram. Eng. Sci. Proc.* **14** [9/10] 824-831 (1993).
13. M. Jones and T.L. Starr, "Enhancements to the Georgia Tech. chemical vapour infiltration process model for ceramic matrix composites", *Ceram. Eng. Sci. Proc.* **16** [5] 829-836 (1995).
14. W.J. Lackey, S. Vaidyaraman, G.B. Freeman and P.K. Agrawal, "Technique for monitoring densification during chemical vapour infiltration", *J. Am. Ceram. Soc.* **78** [4] 1131-1133 (1995).
15. T. Yano, K. Budiyanto, K. Yoshida and T. Iseki, "Fabrication of silicon carbide fiber-reinforced silicon carbide composite by hot-pressing", *Fusion Eng. and Design* **41** 157-163 (1998).
16. A. Sayano, C. Sutoh, S. Suyama, Y. Itoh and S. Nakagawa, "Development of a reaction-sintered silicon carbide matrix composite", *J. Nucl. Mater.* **271-272** 467-471 (1999).
17. J. J. Brennan, "Interfacial characterization of a slurry-cast melt-infiltrated SiC/SiC ceramic-matrix composite", *Acta Mater.* **48** 4619-4628 (2000).
18. D. Brewer, "HSR/EPM combustor materials development program", *Mater. Sci. Eng.* **A261** 284291 (1999).
19. H. O. Davies and D. R. Petrak, "Ceramic matrix composites using polymer pyrolysis and liquid densification processing", *J. Nucl. Mater.* **219** 26-30 (1995).

20. J. Gotoh, K. Tsugeki, A. Sakai and H. Nakayama, “Fabrication and mechanical properties of ceramic matrix composites by polymer impregnation and pyrolysis method”, *Proc. 4th Japan Int. SAMPE Symp.* pp. 240-245 (1995).

21. M.F. Gonon and S. Hampshire, “Comparison of two processes for manufacturing ceramic matrix composites from organometallic precursors”, *J. Eur. Ceram. Soc.* **19** 285-291 (1999).

22. Y-W. Kim, J-S. Song, S-W. Park and J-G. Lee, “Nicalon-fibre-reinforced silicon-carbide composites via polymer solution infiltration and chemical vapour infiltration”, *J. Mater. Sci.* **28** 3866-3868, (1993.)

23. S. Casadio, A. Donato, C.A. Nannetti, A. Ortona and M. Rescio, “Liquid infiltration and pyrolysis of SiC matrix composite materials”, *Ceram. Trans.* **58** 193-198 (1995).

24. S. M. Dong, Y. Katoh, A. Kohyama, S. T. Schwab and L. L. Snead, “Microstructural evolution and mechanical performances of SiC/SiC composites by polymer impregnation/microwave pyrolysis (PIMP) process”, *Ceram. Int.* **28** 899-905 (2002).

25. G. Ziegler, I. Ritcher and D. Suttor, “Fiber-reinforced composites with polymer-derived matrix: processing matrix formation and properties”, *Composites: Part A* **30** 411-417 (1999).

26. G.R. Sherwin, “Non-autoclave processing of advanced composite repairs”, *Int. J. of Adhesion & Adhesives* **19** 155-159 (1999).

27. G. Sala, “Advances in elastomeric tooling technology”, *Materials & Design* **17** [1] 33-42 (1996).

28. M.Z. Berbon, D.R. Dietrich, D.B. Marshall and D.P.H. Hasselman, “Transverse thermal conductivity of thin C/SiC composites fabricated by slurry infiltration and pyrolysis”, *J. Am. Ceram. Soc.* **84** [10] 2229-2234 (2001).

29. A. Timms, W. Westby, C. Prentice, D. Jaglin, R. A. Shatwell and J. G. Binner, “Reducing chemical vapour infiltration time for ceramic matrix composites”, *J. Microsc.*, **201-202** 316-

323 (2001).

30. P. Sarkar, S. Datta and P.S. Nicholson, “Functionally graded ceramic/ceramic and metal/ceramic composites by electrophoretic deposition”, *Composites Part B* **28B** 49-56 (1997).

31. S.N. Heavens, “Electrophoretic deposition as a processing route for ceramics”, *Advanced Ceramic Processing & Technology Vol. I*, pp. 255-283, Ed. J.G.P. Binner, Noyes Publications (1990).

32. A.R. Boccaccini, I. MacLaren and M.H. Lewis, “Electrophoretic deposition infiltration of 2-D woven SiC fibre mats with mixed sols of mullite composition”, *J. Eur. Ceram. Soc.* **17** 1545-1550 (1997).

33. A. Borner and R. Herbig, “ESA measurement for electrophoretic deposition of ceramic materials”, *Colloids and Surfaces A: Physicochemical and Engineering Aspects* **159** 439-447 (1999).

34. H.H. Streckert and J.D. Katz, “Microwave densification of electrophoretically infiltrated silicon carbide composite”, *J. Mater. Sci.* **32** 6429-6433 (1997).

35. S. Kooner, J.J. Campaniello S., Pickering and E. Bullock, “Fiber reinforced ceramic matrix composite fabrication by electrophoretic infiltration”, *Ceram. Trans.* **58** 155-160 (1995).

36. D. Jaglin, J. Binner, C. Prentice, R. Shatwell, L. Timms and W. Westby, “SiC_f/SiC fabrication via vacuum bagging, electrophoretic infiltration and microwave enhanced CVI”, 9^{th} Eur. Conf. on Composite Materials (ECCM 9) proceedings CD, Institute of Materials, Minerals and Mining, UK (2000).

37. A. P. Philipse, “Non-darcian airflow through ceramic foams”, *J. Am. Ceram. Soc.*, **74** [4] 728-732 (1991).

38. T. L. Starr and N. Hablutzel, ‘‘Measurement of gas transport through fiber preforms and densified composites for chemical vapour infiltration,’’ *J. Am. Ceram. Soc.* **81** [5] 1298–304 (1998).

39. J. Binner, B. Vaidhyanathan and D. Jaglin, “Microwave heated chemical vapour infiltration of SiC powder impregnated SiC fibre preforms”, Advances in Applied Ceramics: Structural, Functional and Bioceramics, *In Press*.

Captions

Fig. 1: SEM images of SiC_f/SiC composites processed by CVI (a) low magnification showing large intertow voids and (b) high magnification showing fine intratow porosity. 72 x 72 dpi

Fig. 2: Schematic diagrams showing (a) the vacuum bagging equipment and (b) the electrophoretic impregnation system. 72 x 72 dpi

Fig. 3: Design variations for the anode used for EPI of SiC powder from suspension onto SiC fabric layers. 72 x 72 dpi

Fig. 4a: Reduction in porosity observed in the VB preforms as a function of the solids loading in the SiC slurries. 72 x 72 dpi

Fig. 4b: Reduction in porosity observed in the VB preforms as a function of the particle size in the SiC slurries. 72 x 72 dpi

Fig. 5: SEM cross sectional micrographs of preforms prepared by VB at two different magnifications (a) and (c) V/30/6, (b) and (d) V/20/6. 72 x 72 dpi

Fig. 6: Colour enhanced DEXA scans for samples prepared by a) VB, b) EPI using the vertical electrode and c) combined VB and EPI using the horizontal electrode. 72 x 72 dpi

Fig. 7: Reduction in porosity versus (voltage×time) applied during the EPI process using the vertical electrode. 72 x 72 dpi

Fig. 8: Low and high magnification SEM images of cross sections of preforms formed by EPI (a) and (b) E/5/6-50/90† and (c) E/5/6-100/45. 72 x 72 dpi

Fig. 9: Reduction in porosity versus deposition time for EPI using the vertical (V) and horizontal (H) electrodes and different SiC particle sizes. 72 x 72 dpi

Fig. 10: Low and high magnification SEM images of cross sections of preforms formed by combined VB and EPI (a) and (b) EV/5/25-50/60; (c) and (d) EV/5/67-50/60 and (e) and (f) EV/5/100-50/60. 72 x 72 dpi

Table I: Mean particle size and source of SiC particles used.

Table II: Impregnation results achieved by the VB process.

Table III: Impregnation results achieved by the EPI process.

Table IV: Impregnation results achieved by the combined horizontal EPI and VB processes and the combined horizontal GS and VB processes.

Table I: Mean particle size and source of SiC particles used.

Mean particle size / μm	Source
0.6	UF15, HC Starck, Goslar, Germany
2.5	ESK1500F, ESK, Kempten, Germany
6.7	Reliable Techniques, Newcastle-under-Lyme, UK
10.0	Carborex BW Micro F 600 PV, Washington Mills Electro Minerals, Manchester, UK
12.8	Silkaride CS F1200, Washington Mills Electro Minerals, Manchester, UK

Table II: Impregnation results achieved by the VB process.

Sample	Slurry type	Solid loading / %	Particle size / μm	V_f / %	V_p / %	V.R. / %	Relative density / %	Gas permeability[#] / 10^{-12} m^2
V/20/6	A	20	0.6	25	9	12	34	*
V/20/25	A	20	2.5	23	6	10	29	*
V/20/128	A	20	12.8	21	8	11	29	*
V/30/6	A	30	0.6	35	15	23	50	*
V/30/100	A	30	10.0	14	15	17	29	1.3
V/35/6	A	35	0.6	21	18	23	39	2.0
V/35/25	A	35	2.5	19	16	28	35	1.9
V/35/67	A	35	6.7	16	19	23	35	1.8
V/35/100	A	35	10.0	18	21	26	39	1.1
V/40/100	A	40	10.0	16	21	25	37	1.0

[#]16×10^{-12} m^2 for a powderless preform
*Technique not available at the time

Table III: Impregnation results achieved by the EPI process.

Sample	Slurry type	Solid loading / %	Particle size / μm	Electrode type	Voltage / V	Time / s	V_f / %	V_p / %	V.R. / %	Relative density / %
E/5/6-50/45†	B	5	0.6	Vertical	50	45	21	7	9	28
E/5/6-50/60	B	5	0.6	Vertical	50	60	17	15	18	32
E/5/6-50/90	B	5	0.6	Vertical	50	90	16	18	21	34
E/5/6-50/90†	B	5	0.6	Vertical	50	90	22	12	15	34
E/5/6-100/45	B	5	0.6	Vertical	100	45	20	19	24	39
E/5/25-50/60	B	5	2.5	Vertical	50	60	20	11	14	31
E/5/25-100/30	B	5	2.5	Vertical	100	30	22	13	17	35
E/5/25-100/60	B	5	2.5	Vertical	100	60	19	21	26	40
E/10/25-50/60	B	10	2.5	Vertical	50	60	18	26	32	44
E/5/25-50/60	B	5	2.5	Horizontal	50	60	18	12	15	30

† Alternate layers impregnated

Table IV**:** Impregnation results achieved by the combined horizontal EPI and VB processes and the combined horizontal GS and VB processes.

Sample	Slurry type	Solid loading / %	Particle size / μm	V_f / %	V_p / %	V.R. / %	Relative density / %	Gas permeability / 10^{-12} m^2
EV/5/25-50/60	C	5	2.5	18	17	21	35	6.9
EV/5/67-50/60	C	5	6.7	21	18	23	39	6.8
EV/5/100-50/60	C	5	10	21	19	24	40	6.3
GV/5/67-B	B	5	6.7	17	19	23	36	12.8
GV/5/67-C	C	5	6.7	19	22	27	41	6.8
GV/5/100-B	B	5	10	21	20	25	41	10.6
GV/5/100-C	C	5	10	20	20	25	40	6.0

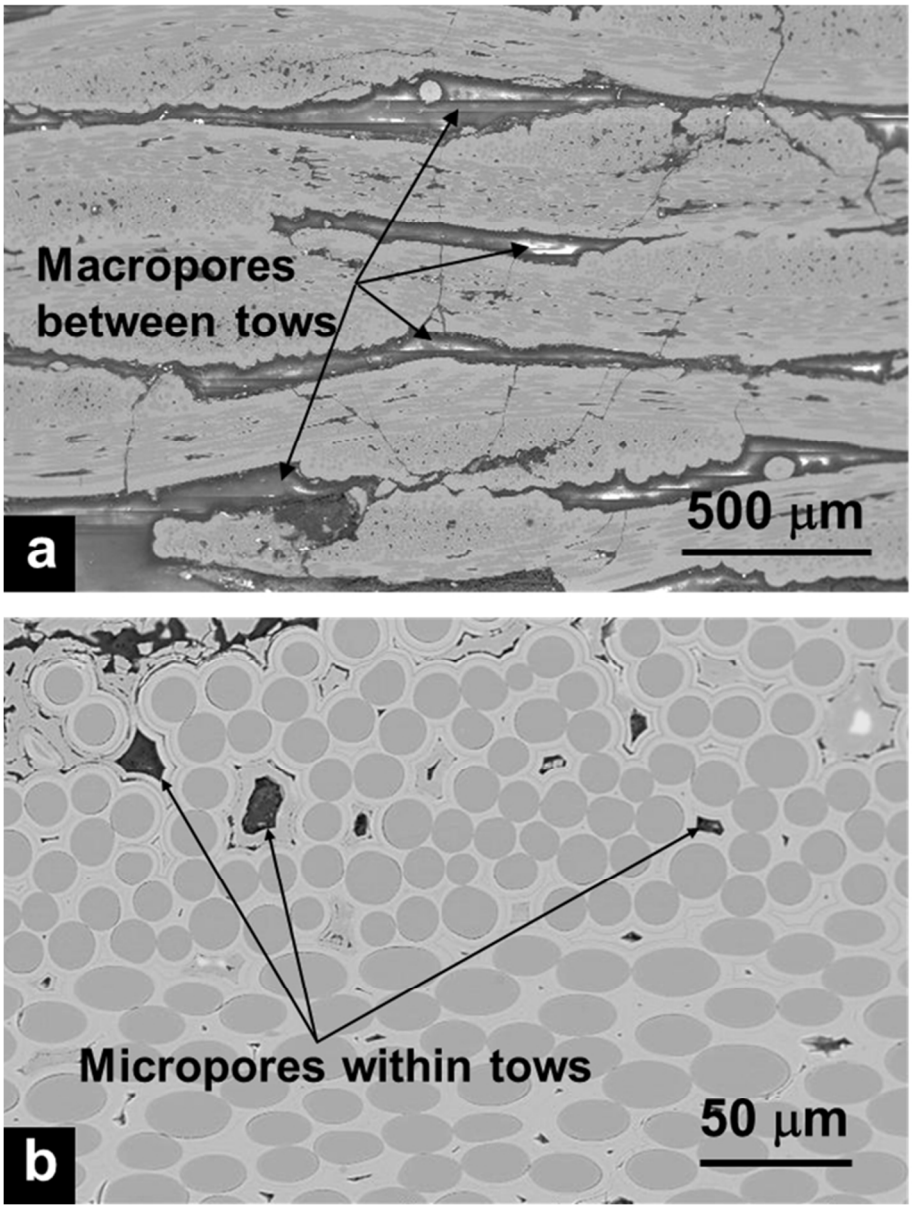

Fig 1. SEM images of SiCf/SiC composites processed by CVI (a) low magnification showing large intertow voids and (b) high magnification showing fine intratow porosity. 72 x 72 dpi

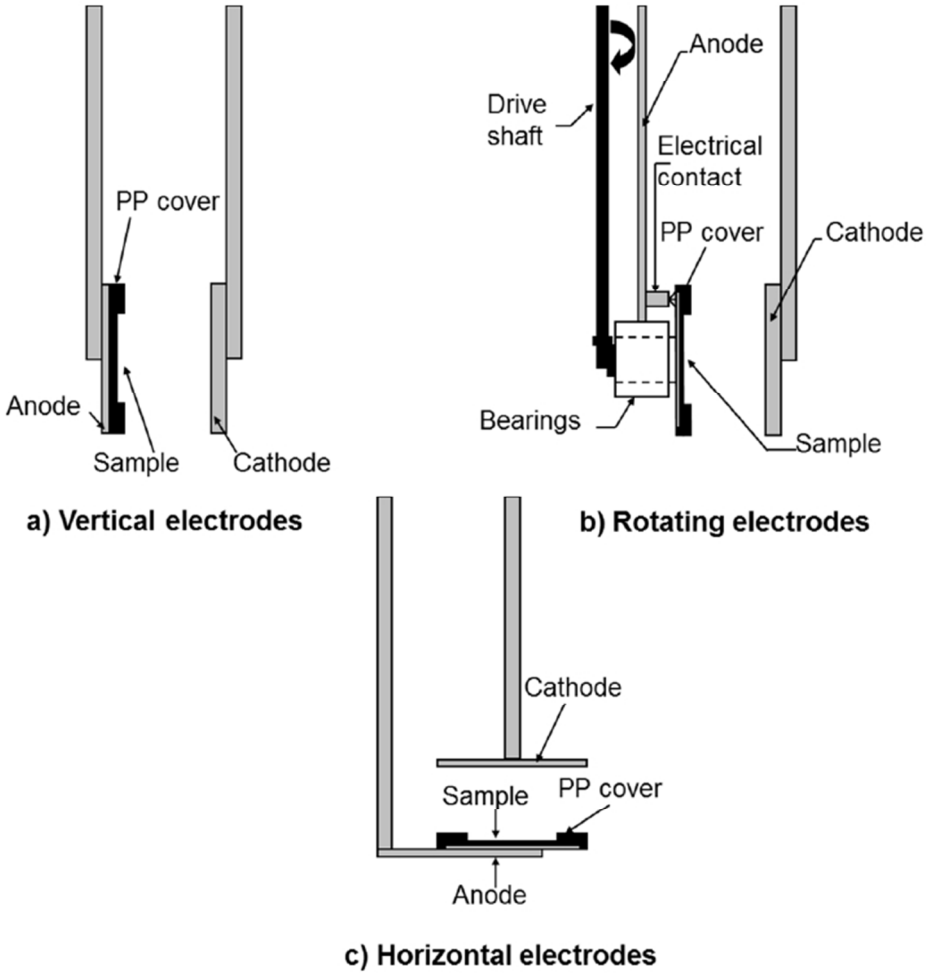

Fig 3. Design variations for the anode used for EPI of SiC powder from suspension onto SiC fabric layers. 72 x 72 dpi

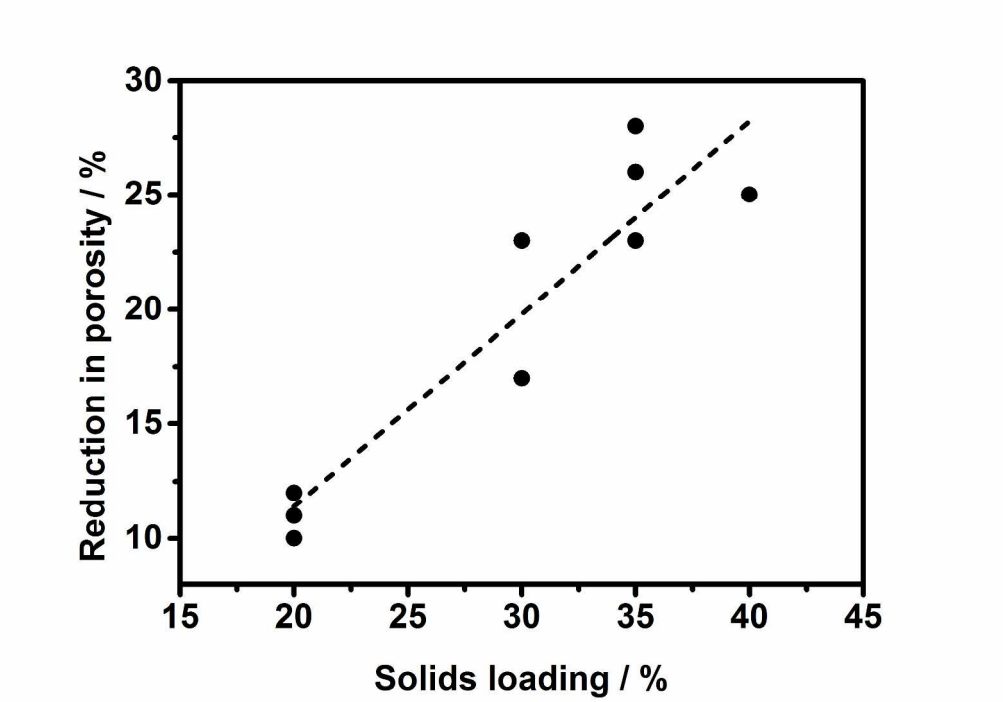

Reduction in porosity observed in the VB preforms as a function of the solids loading in the SiC slurries. 72 x 72 dpi
287x201mm (300 x 300 DPI)

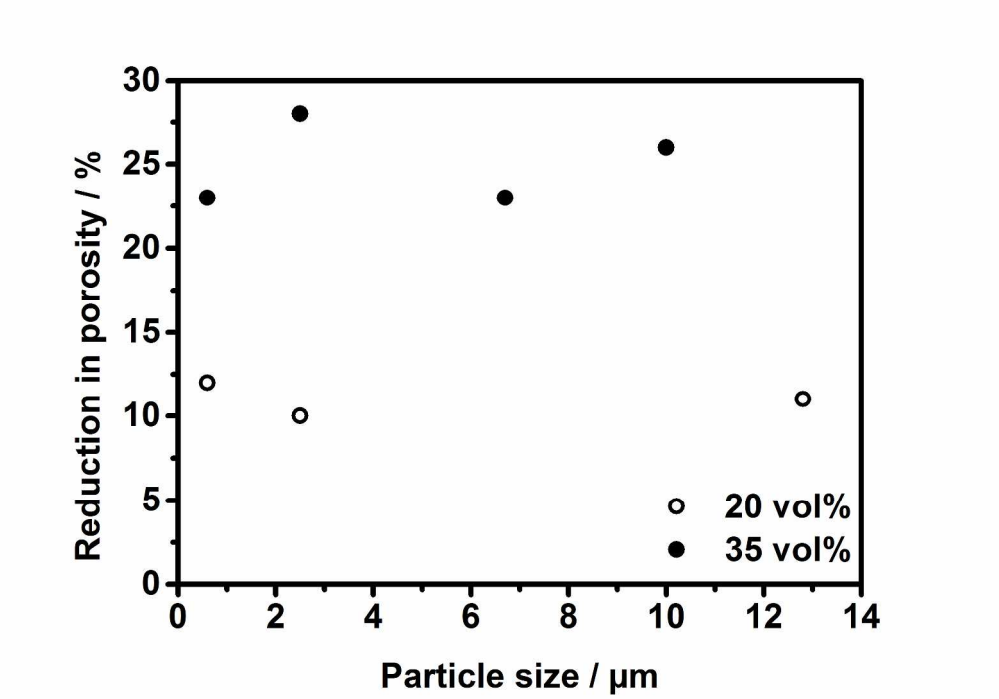

Reduction in porosity observed in the VB preforms as a function of the particle size in the SiC slurries. 72 x 72 dpi
287x201mm (300 x 300 DPI)

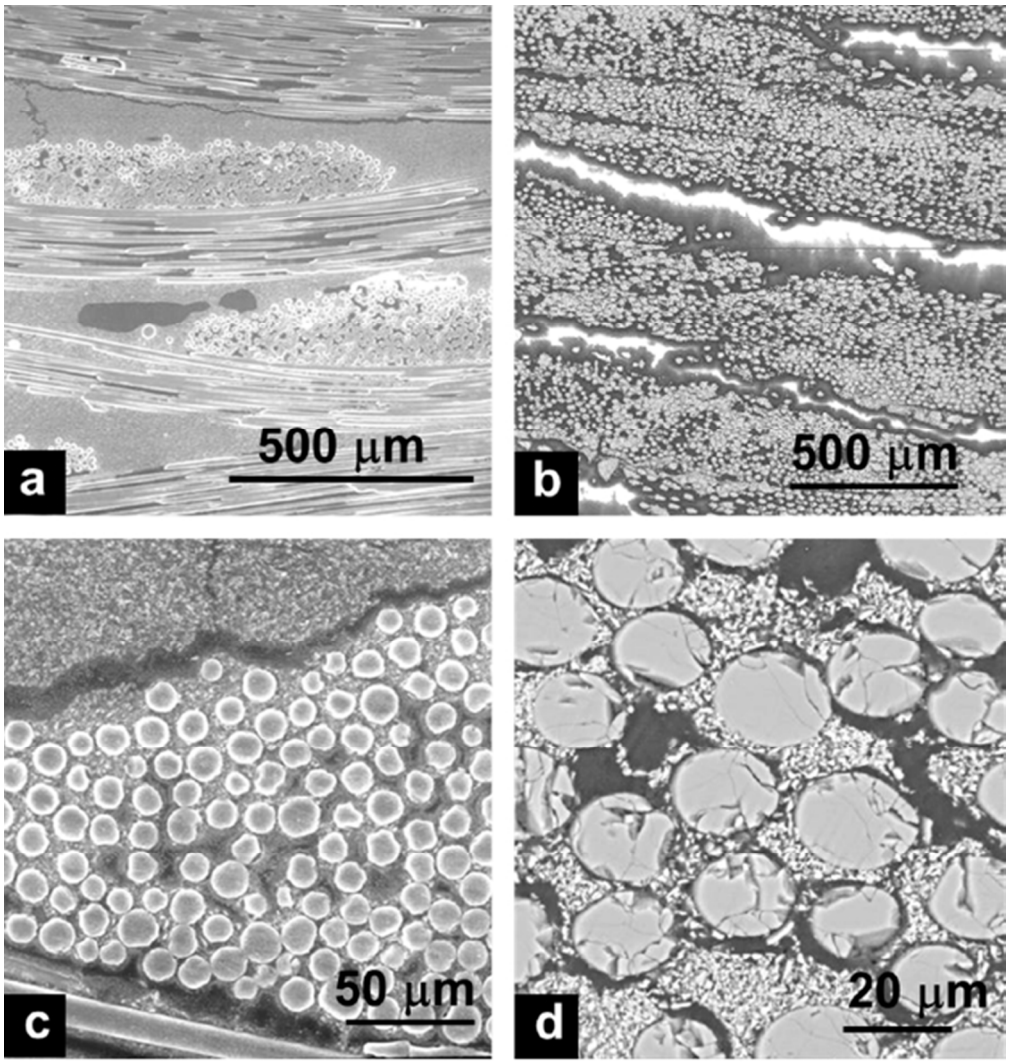

Fig 5. SEM cross sectional micrographs of preforms prepared by VB at two different magnifications (a) and (c) V/30/6, (b) and (d) V/20/6. 72 x 72 dpi

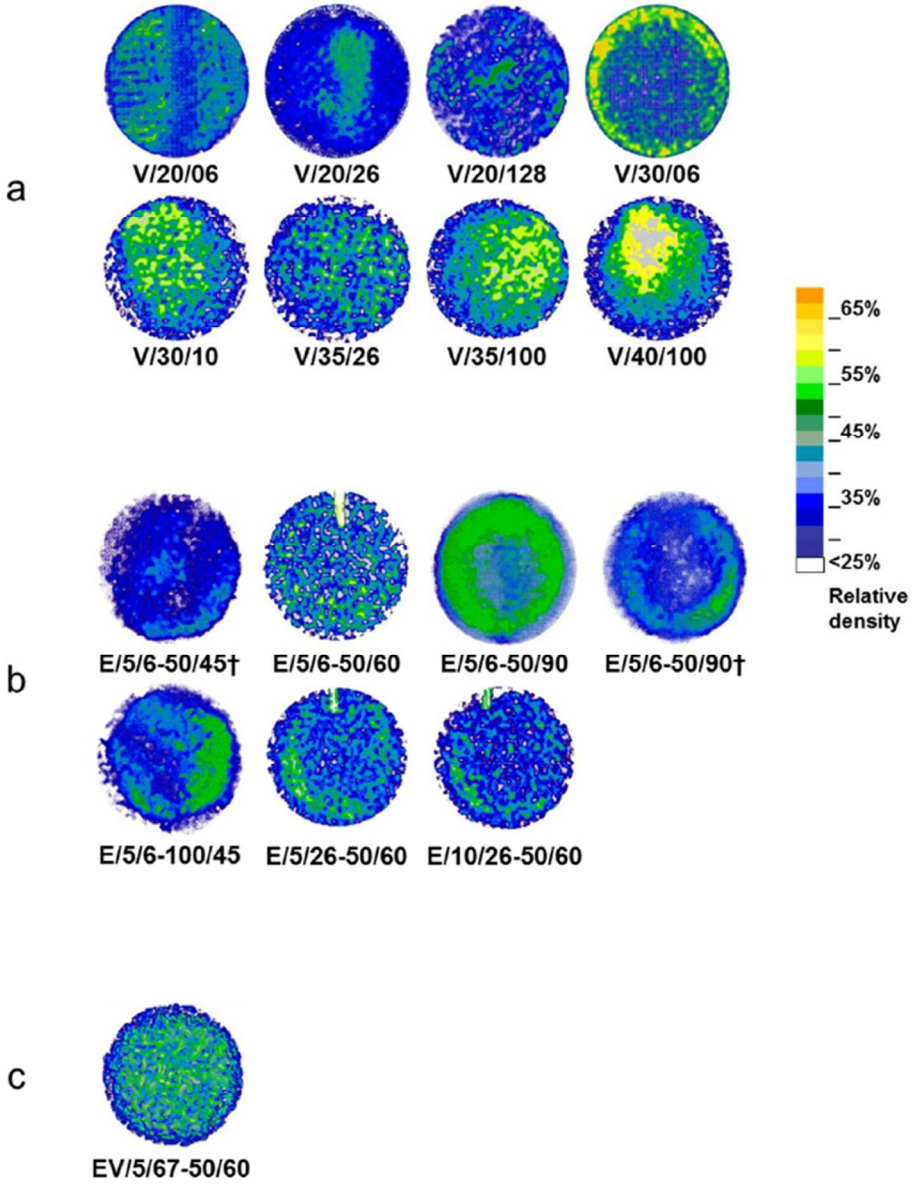

Fig 6. Colour enhanced XRA scans for samples prepared by a) VB, b) EPI using the vertical electrode and c) combined VB and EPI using the horizontal electrode. 72 x 72 dpi

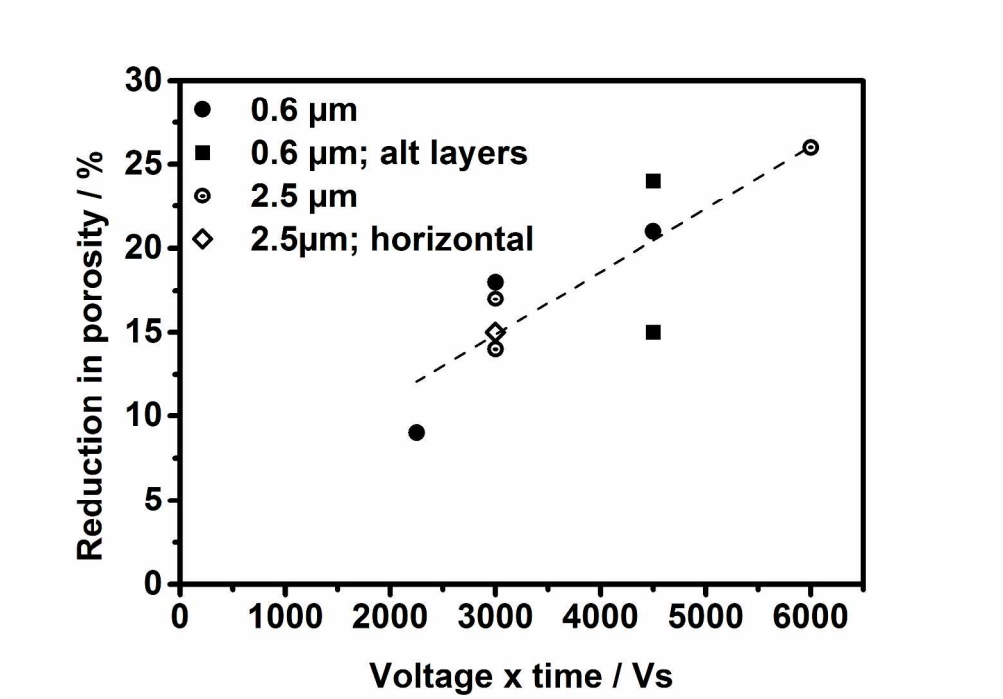

Reduction in porosity versus (voltage×time) applied during the EPI process using the vertical electrode. 72 x 72 dpi
287x201mm (300 x 300 DPI)

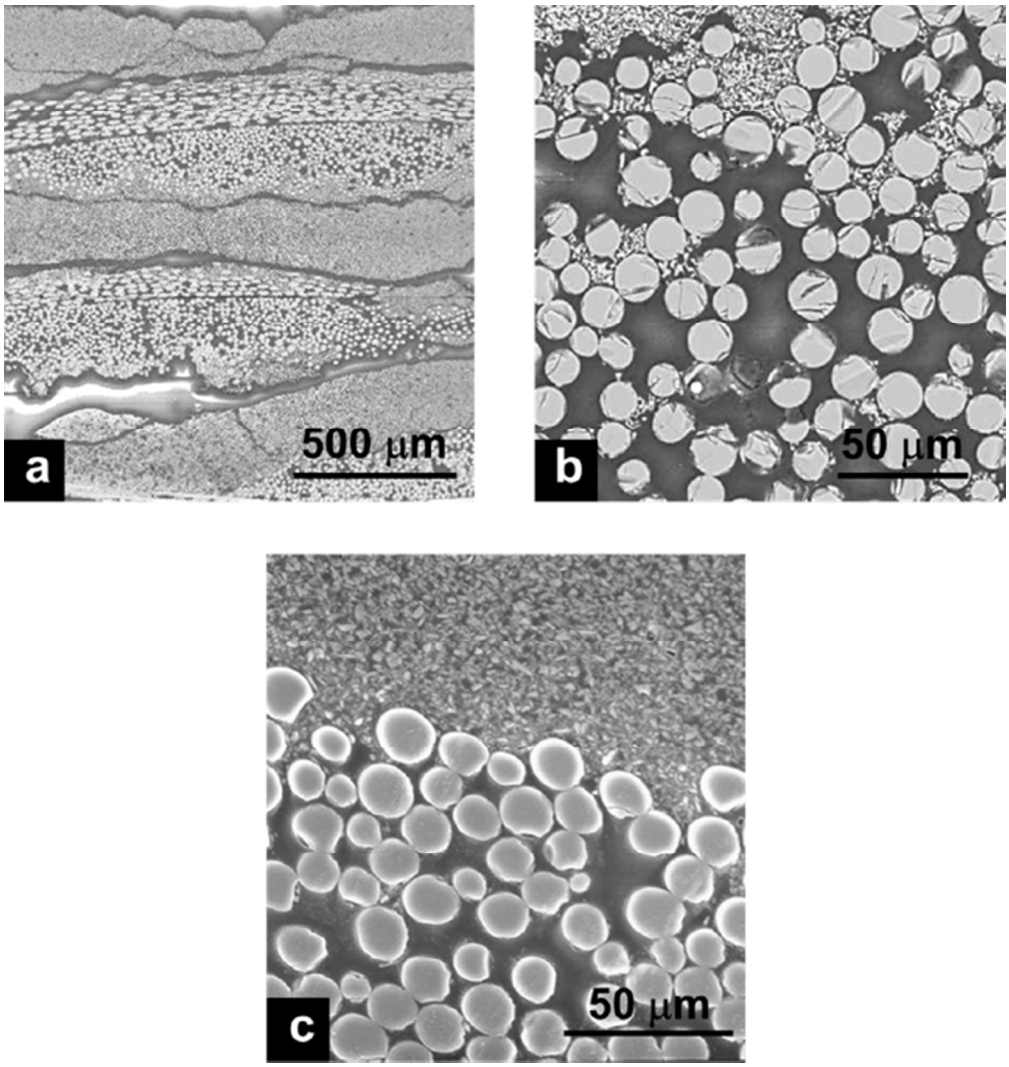

Fig 8. Low and high magnification SEM images of cross sections of preforms formed by EPI (a) and (b) E/5/6-50/90† and (c) E/5/6-100/45. 72 x 72 dpi

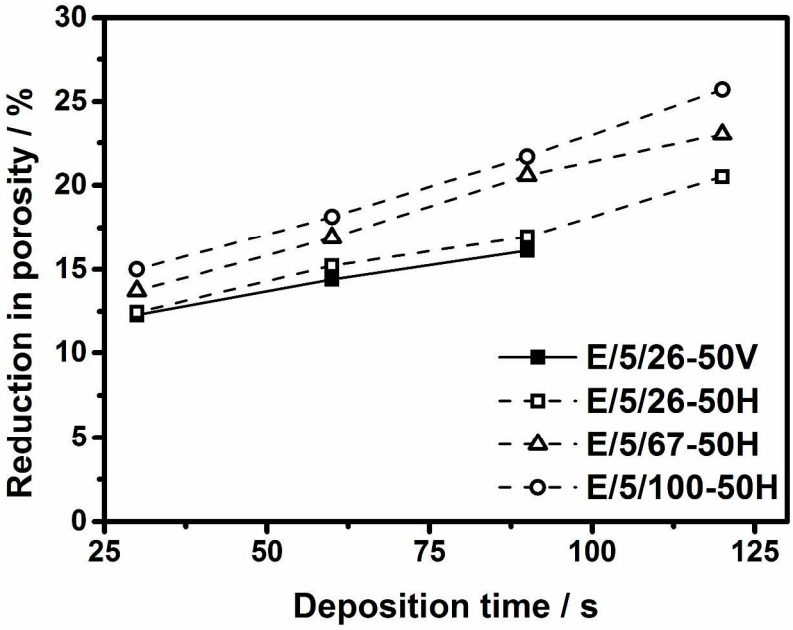

Reduction in porosity versus deposition time for EPI using the vertical (V) and horizontal (H) electrodes and different SiC particle sizes. 72 x 72 dpi
287x201mm (300 x 300 DPI)

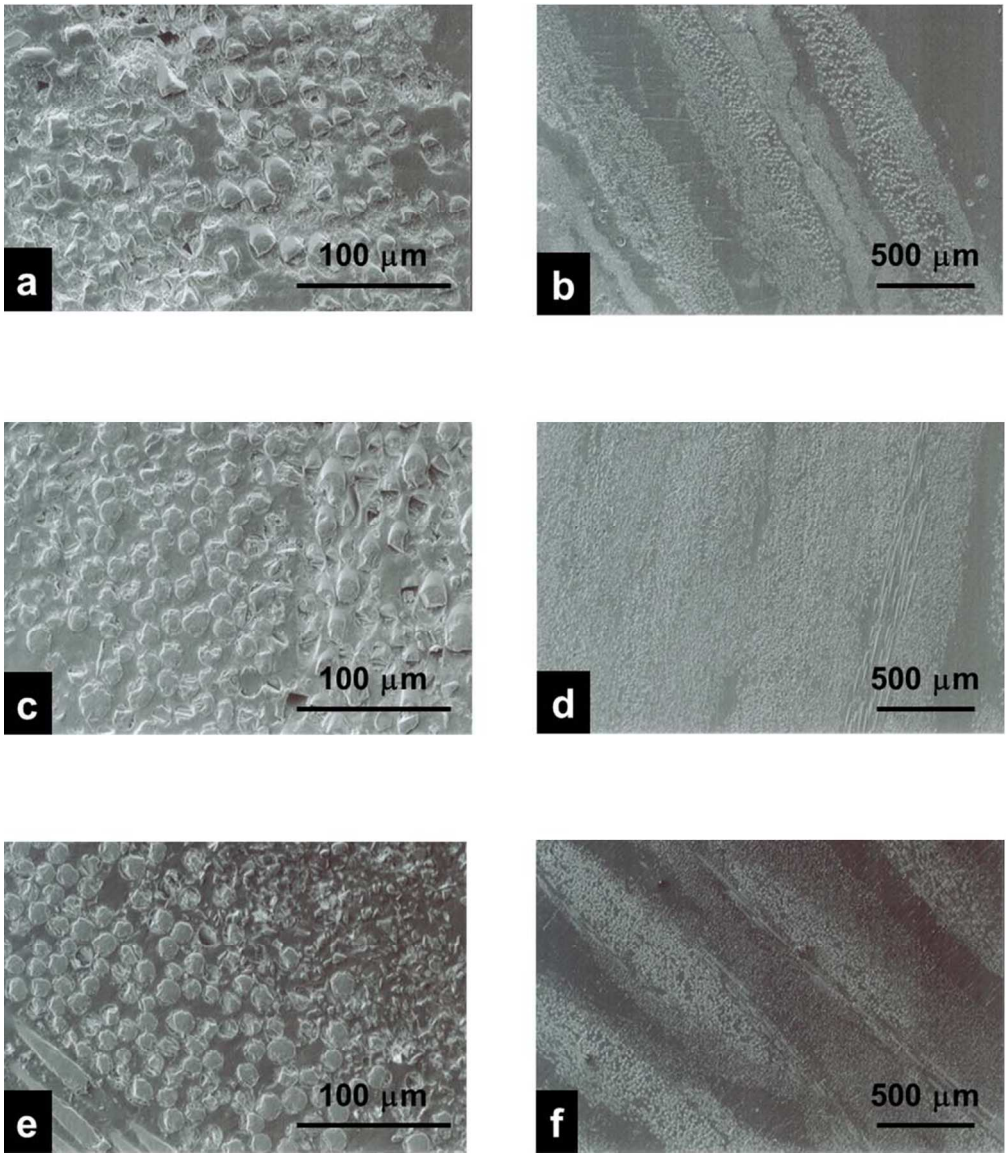

Fig 10. Low and high magnification SEM images of cross sections of preforms formed by combined VB and EPI (a) and (b) EV/5/25-50/60; (c) and (d) EV/5/67-50/60 and (e) and (f) EV/5/100-50/60. 72 x 72 dpi